ALMA MATER STUDIORUM
UNIVERSITÀ DI BOLOGNA

DOTTORATO DI RICERCA IN

Oncologia, Ematologia e Patologia

Ciclo **XXXVI**

Settore Concorsuale: 06/A4

Settore Scientifico Disciplinare: MED/08

TITOLO TESI

Bright-Field Multiplex Immunohistochemistry for Tumor Microenvironment Evaluation in Mucosal Melanoma of the Head and Neck Region: Technical Aspects, Results, and Correlation with Clinicopathologic Features and Molecular Landscape

Presentata da: *Costantino Ricci*

Coordinatore Dottorato

Prof.ssa Manuela Ferracin

Supervisore

Prof. Michelangelo Fiorentino

Co-supervisore

Prof.ssa Maria Pia Foschini

ALMA MATER STUDIORUM
UNIVERSITÀ DI BOLOGNA

Esame finale anno 2024

ALMA MATER STUDIORUM
UNIVERSITÀ DI BOLOGNA

Summary

ALMA MATER STUDIORUM
UNIVERSITÀ DI BOLOGNA

ALMA MATER STUDIORUM
UNIVERSITÀ DI BOLOGNA

1. Abstract

Mucosal melanoma of the head and neck region (MM-H&N) is a rare disease, characterized by a poor prognosis and limited therapeutic strategies, especially regarding targeted therapy (lower rate of targetable mutations compared to cutaneous melanoma) and immunotherapy (lack of diagnostic tools able to predict the response). Meanwhile, bright-field multiplex immunohistochemistry (BF-mIHC) is emerging as a promising tool for characterizing tumor microenvironment (TME) and predicting response to immunotherapy in several tumors, including melanoma. This PhD project aims to develop a BF-mIHC protocol to evaluate the TME in MM-H&N, analyze the correlation between immune markers/immune profiles and MM-H&N features (clinicopathologic and molecular), and find new biomarkers useful for prognostic-therapeutic stratification of these patients. Specific aims are: (I) describe the clinicopathological features of MM-H&N; (II) analyze the molecular status of MM-H&N and correlate it with the clinicopathological features; (III) analyze the molecular status of multiple specimens from the same patient to verify whether molecular heterogeneity of MM-H&N could affect the results with relevant prognostic-therapeutic implications; (IV) develop a BF-mIHC protocol to study TME in MM-H&N; (V) analyze the correlation between immune markers/immune profiles and MM-H&N features (clinicopathologic and molecular) to test whether BF-mIHC could be a promising tool for prognostic-therapeutic characterization of these patients.

2. Introduction

2.1 Epidemiology

The USA Cancer Database reported that mucosal melanoma (MM) represents approximately 1.3% of all melanomas [1]. About 40-55% of all MM arise in the head and neck area (MM-H&N), with the majority originating in the nasal cavity/nasal septum/turbinates (NC/NS/T) (70%) followed by the oral cavity, namely tongue and palate (20%) [1-4]. The median age at diagnosis for MM-H&N is about 60 years, with discordant results about the sex prevalence and both male and female preponderances reported for NC/NS/T MM-H&N [1-4]. Recent studies and meta-analyses reported a trend toward an increasing incidence of MM-HN, albeit less pronounced than that of cutaneous melanoma [5, 6]. *Marcus DM et al* found an increase in the incidence of MM-HN in the USA (1987-2009), with an annual percentage change of 2.4%, but exclusively for NC/NS/T MM-H&N [6]. Furthermore, the epidemiology of MM shows remarkable differences among different ethnicities [7-10]. One previous study analyzed the population-based California Cancer Registry (1988-2013) and reported that MM represents only 0.5-1% of all melanomas in non-Hispanic whites, but about 15% in Asian/Pacific Islanders, 9% in non-Hispanic blacks, and 4% in Hispanics [10]. Notably, the highest incidence of MM is recorded in Asian countries; indeed, MM was reported to account for 23% of all melanomas in China, and oral cavity MM-H&N for 7.5% of all melanomas in Japan [7-10].

2.2 Risk factors

The risk factors and pathogenesis of MM-H&N are largely unknown, and there is much less data if compared to its cutaneous counterpart [11-14]. The major difference is that MM-H&N is not associated with sun exposure and UV-signature, which markedly affects the epidemiology, pathogenesis, and molecular landscape of MM-H&N (no C>T transitions UV-induced; exceptionally rare *BRAF p.V600E* and *TERTp* mutations as in low-CSD melanoma, rare bi-allelic inactivating *NF1* and "not-canonical" *BRAF* mutations as in high-CSD melanoma; lower mutational burden if compared to cutaneous melanoma) [15]. At the state-of-the-art, no well-established risk factors have been identified for MM-H&N, but isolated studies reported that inhaled and ingested carcinogens (smoke and formaldehyde), family history, viruses (HPV, HHV 1-2, and polyomavirus), ill-fitting dentures, and pre-existing oral lesions could increase the risk of developing MM-H&N [1-3, 11-14]. MM-H&N originates from melanocytes migrating to the oral cavity, NC/NS/T, and salivary glands from 20-23 weeks of gestation [14]. It has been speculated that the pathogenesis of MM-H&N could be linked to the early phases of this embryonal migration because of the proximity of the most frequently affected H&N sites (lower portion of NC/NS/T, maxillary sinus, hard palate, upper gingiva) [15].

2.3 Biology and pathology

2.3.1 Biology and pathology: molecular landscape

MM-H&N is a rare disease and little is known about its molecular landscape, differently from its cutaneous counterpart for which the amount of literature data is extremely wide and several targeted therapies are available for advanced-stage, unresectable, and metastatic cases [15-33]. Cutaneous melanoma can be divided into four molecular subgroups [*BRAF*-mutated, *NRAS*-mutated, *NF1*-

mutated, and triple wild-type (WT)] with marked clinicopathological differences [33]. Specifically, the latest World Health Organization (WHO) Classification of Skin Tumours (fifth edition, 2023) introduced a combined (clinicopathologic and molecular) classification of melanocytic lesions based on the degree of sun damage (low- and high-CSD) and reflected in divergent molecular landscape, epidemiology, clinicopathological features [33]. By contrast, the molecular landscape of MM-H&N is largely uncharacterized [15-33]. The first studies adopted Sanger sequencing limited to few genes (*BRAF*, *KIT*, and *NRAS*), whereas very recent ones utilized detailed and combined approaches [targeted and whole DNA- and RNA-next-generations sequencing (NGS) panels, PCR, FISH, and Sanger sequencing)] partially limited by high costs preventing their routine application, and by the finding of "non-canonical" mutations with prognostic-therapeutic implications not well-known in melanoma [15-33]. Besides, the low number of cases and the marked heterogeneity of the analyzed case series (MM vs MM-H&N; NC/NS/T vs oral cavity; Asian patients vs European and American patients; primary vs metastatic cases) contributed to fragmentation and partial obfuscation of the molecular data in this melanoma subtype [15-33]. What is certainly known is that sun damage's role is almost completely absent in MM-H&N, and this data reflects its molecular landscape: a) no/paucity of UV-signature (C>T transition); b) low frequency of UV-induced mutations (*BRAF p.V600E*, *TERTp*, *NF1*, "not-canonical" *BRAF* mutations, etc.); c) lower mutational burden than its cutaneous counterpart [15-33]. The most frequently involved genes in the pathogenesis of MM-H&N are *NRAS* and *KIT* but with mutation rates deeply varying among the different studies (range: 0-55% for both genes), followed by a large plethora of rarely mutated genes (*SF3B1*, *TP53*, *GNAQ*, *GNA11*, *KRAS*, etc.) [15-33]. Very curiously, although with different frequencies and not UV-induced, the molecular profile of MM (and MM-H&N) is more similar to

that of high-CSD (*NF1*, *KIT*, *NRAS*, and "not canonical" *BRAF* mutations) than low-CSD (*BRAF p.V600E* and *TERTp* mutations) melanoma [15-33]. The majority of previous studies and recent reviews suggest the predominant role of *NRAS* vs *KIT* oncogenesis in NC/NS/T MM-H&N, with a reverse correlation for oral cavity MM-H&N (predominant *KIT* oncogenesis) [16, 17, 19, 21, 24, 25, 30, 32]. However, other studies failed to confirm these findings and reported results contrasting with this "molecular status-site" correlation, probably due to the above-mentioned reasons (heterogeneity in case series and molecular tests) and combination of cases from NC/NS/T and oral cavity in a single "H&N category" [18, 20, 22, 27-29]. Besides, the correlation between specific mutations and clinicopathologic features, prognosis, and response to therapies in MM-H&N is still lacking and/or contrasting among different studies [15-33]. As a result, our knowledge of the molecular landscape of MM-H&N is partial and results in significant limitations of therapeutic strategies, also considering the availability of targeted therapies (NRAS-, BRAF-, KIT-, and MEK-inhibitors) in advanced-stage, unresectable, and metastatic cases [15-33]. In this PhD project, we aimed to analyze the molecular status of MM-H&N and correlate it with clinicopathological features, focusing on multiple specimens obtained from the same patient to verify whether molecular heterogeneity of MM-H&N could affect the results with relevant prognostic-therapeutic implications.

2.3.2 Biology and pathology: tumor microenvironment and future perspectives with multiplexing

Tumor microenvironment

Tumor-infiltrating lymphocytes (TILs) are a crucial component of tumor microenvironment (TME) and are frequently observed in different tumors, including cutaneous and mucosal melanoma [34-43]. Their presence is generically considered a favorable prognostic factor in melanoma, regardless of the lymphocyte subclass (CD3, CD20, CD8, etc.), histologic subtype, and pT stage [33, 37-41]. Besides, other cells [tumor-associated macrophages (TAMs), fibroblasts, endothelial cells, etc.] cooperate with TILs in establishing TME of melanoma, each of them with specific roles in its biology and different clinicopathological implications [33, 37-41]. However, the real impact of TILs, TAMs, and TME on prognosis and therapy [especially for immune checkpoint inhibitors (ICIs)], as well as the modality to investigate and report (qualitative or quantitative methods? Direct visual or analogic visualization? Which lymphocyte subclasses? Peri-tumoral or intra-tumoral evaluation?) are not well-established [33, 37-41]. This is a crucial limitation for the adoption of ICIs, which nowadays represent the standard-of-care for the treatment of unresectable and metastatic melanoma [40, 41]. Historically, TME in tumors (and in cutaneous melanoma) has been classified into four different subtypes, based on TILs and programmed death-ligand 1 (PD-L1) expression: type I-adaptive immune resistance, type II-immunological ignorance, type III-intrinsic induction, type IV-tolerance, with different response rates to ICIs and outcome [44]. Subsequently, tumor classification based on the distribution of immune markers, namely “hot”/inflamed, “cold”/desert, and “cold”/excluded, proved to correlate with prognosis and response to ICIs in different tumors including melanoma [41]. Combined classification schemes adopting tumor mutational burden (TMB) and gene expression profile (GEP) predicted response to ICIs and prognosis in several tumors, thus resulting in an expensive but promising tool for planning the therapy [41, 45]. However, despite the massive efforts of the scientific community, at the state-of-

the-art, no diagnostic tools are reliably able to identify responder patients, characterize mechanisms of resistance, and predict toxicity to ICIs [39-41, 45]. As a result, in the current National Comprehensive Cancer Network (NCCN) 2023 melanoma guidelines, PD-L1 immunocytochemistry, TMB, and GEP tests are not recommended for administering ICIs and should not guide clinical decisions [46]. Furthermore, these data and the corresponding guidelines have been obtained in cutaneous melanoma and *bona fide* transferred to MM and MM-H&N [15, 33, 37, 40, 41, 46-49]; however, clinical trials focused on ICIs in MM (but not specifically in MM-H&N) have been developed or are ongoing [15, 33, 37, 40, 41, 46-49]. *Ledderose S et al* showed that TILs were associated with increased overall survival (OS), and brisk TILs with lower pT stage and increased recurrence-free survival (RFS) and 5-year survival (5y-S) in "sino-nasal" melanoma [42, 43]. The same working group found that high levels of CD3 and CD8 were associated with lower pT stage, and increased OS and 5y-S in "sino-nasal" melanoma [42, 43].

Multiplexing

Historically, pathologists analyzed TME and TILs in melanoma tissues on hematoxylin and eosin (H&E) slides and with immunohistochemistry (IHC) for specific markers (CD20, CD3, CD4, CD8, CD16, CD163, FoxP3, PD-L1) [37-39]. The advantages of these well-established methods are the fast times, readily available, low cost, the possibility to evaluate cell density and location (intra-tumoral and peri-tumoral), as well as the greater familiarity of pathologists with light microscopy compared to other techniques [37-39]. However, visual direct interpretation is affected by low interobserver reproducibility and the need to visualize different cells in consecutive sections, making it difficult to compare cells to each other [37-39]. Multiplexing [bright-field multiplex

immunohistochemistry (BF-mIHC) and multiplex immunofluorescence (mIF)] has emerged as a revolutionary diagnostic tool to characterize TME, allowing the simultaneous detection of ≥ 2 markers in a single section and an in-depth characterization of the TME [50-52]. Multiplexing has become useful assays in research investigations and proved to be better performing than other methods (TMB, standard IHC, GEP, etc.) for predicting the response to ICIs of several tumors [50-52]. Furthermore, several issues (times, costs, expertise, choice of the immune markers to investigate, etc.) and methodological aspects (chromogens and fluorophores, visualization and score systems, etc.) still deserve to be clarified [50-52]. Two of the most crucial aspects are visualization and score systems [50-52]. The approach for interpreting BF-mIHC and mIF could vary depending on the adopted technique and the main target of the analysis [50-52]. Direct visual interpretation by a pathologist (glass slide for BF-mIHC and digitized slide for mIF) could be sufficient for easy and straightforward tasks, such as TME immunophenotyping [50-52]. More sophisticated analyses (quantitative-spatial profiling, cellular density, and spatial relationships between cell types) may require digital analyses and dedicated software. In conclusion, although multiplexing offers unprecedented opportunities for elucidating biology and guiding the therapy of melanoma, several aspects need to be still clarified [50-52]. In this PhD project, we aimed to characterize TME in MM-H&N using a low-plex four-label BF-mIHC protocol (CD3, CD20, CD68, and SOX10), visual direct interpretation, and "*easy-to apply*" score (previously tested by our group, familiar to pathologists, and not requiring sophisticated instrumentation) to analyze the correlations between immune markers (CD3, CD20, and CD68) and clinicopathological features or molecular landscape in MM-H&N.

2.4 Diagnosis

2.4.1 Diagnosis: signs and symptoms

Clinical signs and symptoms at diagnosis depend by the site [47-49, 53-55]. In NC/NS/T MM-H&N, signs and symptoms at diagnosis (epistaxis, facial pain, nasal obstruction, and discharge) are not specific and it could be misdiagnosed as an inflammatory condition [47-49, 53-55]. By contrast, more specific signs and symptoms (skin infiltration and ulceration, exophthalmos, ophthalmoplegia, etc.) are usually observed in advanced-stage cases [47-49, 53-55]. Oral cavity MM-H&N is a variably-pigmented (frequently presenting as bluish colored nodule) and asymptomatic (except for advanced-stage cases showing ulceration and hemorrhage) lesion, but usually diagnosed earlier than NC/NS/T MM-H&N due to greater accessibility for clinical exams [56, 57]. Furthermore, up to 10-30% of oral cavity MM-H&N are amelanotic with a more challenging diagnosis [56, 57]. In MM-H&N of other sites (hypopharynx, nasopharynx, oropharynx, larynx, maxillary sinus, etc.), the clinical presentation does not differ from other tumors (squamous cell carcinoma, sarcomas, salivary gland tumors, etc.) and encompass hoarseness, dysphagia, dysphagia, and dyspnea [58, 59]. Local recurrence and/or residual tumor at the surgical site is extremely common in MM-H&N due to the peculiar anatomical conditions that favor infiltration of relevant anatomical structures and discourage aggressive surgery [47-49, 53-59]. For the same reasons, as well as issues related to surgical approaches, local recurrence and/or residual tumor is much more common in NC/NS/T than in oral cavity MM-H&N [47-49, 53-59]. The risk of lymph-node involvement at diagnosis is higher in the oral cavity (25-40%) rather than NC/NS/T MM-H&N (<10%), and previous studies found that clinicopathologic features associated with an increased risk: a) diameter > 4 cm; b) nodular histotype; c) depth of invasion > 5 mm [47-49, 53-59]. For these reasons, some authors

suggested elective neck dissection in MM-H&N with these features, and close observation in the other cases [47-49, 53-59]. The occurrence of distant metastases at diagnosis (mainly brain and lungs) is about 5-10% with no discrepancies among different sites, even if some authors reported a higher percentage in NC/NS/T cases [47-49, 53-59]. The risk of lymph-node and distant metastases increases over the years, especially in case of local recurrence and/or residual tumor [47-49, 53-59].

2.4.2 Diagnosis: imaging

The gold standard for the radiological diagnosis of MM-H&N is the 3-D magnetic resonance imaging (MRI), allowing an accurate delineation of the site and extension of the tumor, as well as the relationships with all the surrounding anatomic structures [47-49, 60, 61]. The MRI signal in MM-H&N is strongly influenced by the amount of melanin and hemorrhage (intrinsic paramagnetic properties and free radicals produced by the interaction with the metals) and accounts for a mixed pattern composed of T1-hyperintensity and T2-hypointensity [47-49, 60, 61]. However, the rarity of MM-H&N limits the collection of large case series and the detailed collection of MRI data on this entity [47-49, 60, 61]. Recent studies showed that the apparent diffusion coefficient measured with diffusion-weighted sequences could be a promising MRI parameter for the radiologic diagnosis of MM-H&N, but the amount of data is still limited and future studies are needed to verify its effective diagnostic potential [47-49].

2.4.3 Diagnosis: WHO classification and histology

In the latest WHO Classification of Head and Neck Tumours (5th edition, 2022), MM-H&N is defined as a "malignant neoplasm of mucosal melanocytes" [15]. MM-H&N has distinct clinicopathologic, prognostic, and molecular features depending on the site (NC/NS/T, oral cavity, pharynx, etc.) and it may be simplistic to group them all as one disease [15, 47-49]. However, there is a single chapter for MM-H&N in the latest WHO edition, due to similar histologic features regardless of site [15]. The WHO recognizes three main histologic subtypes (nodular, mucosal lentiginous, and desmoplastic) and three main cellular phenotypes (epithelioid, fused, and mixed) [15]. Histologic diagnosis of MM-H&N on surgical resections (excision of primary tumor and excision of local recurrence and/or residual tumor) could be straightforward for pathologists specialized in H&N pathology [15]. MM-H&N is characterized by nodular, solid, diffuse, and/or fascicular proliferation of highly atypical melanocytes (pleomorphic and densely packed cells, prominent nucleoli, mitoses, and apoptotic bodies) with variable cellular phenotypes (epithelioid, spindle, plasmacytoid, and mixed) [15]. MM-H&N usually shows ulceration, necrosis, lympho-vascular invasion, perineural infiltration, bone and/or cartilage involvement, and a destructive pattern [15]. Furthermore, immunohistochemical analysis is always required to confirm the melanocytic nature of the lesion and to differentiate it from potential histologic mimickers (sarcomas, squamous cell carcinomas, salivary gland tumors, metastases, etc.) and it is based on the expression of melanocytic markers commonly adopted for its cutaneous counterpart (MiTF, S-100, HMB45, Melan A, and SOX10) [15, 62]. Due to possible negative staining for these markers, it is strongly recommended to use more than one and in combination with other lineage markers (cytokeratin cocktail, specific mesenchymal lineage markers, etc.) [15, 62]. In not uncommon clinical scenarios (poorly cellular incisional biopsies, fragmented and/or necrotic specimens, etc.),

the diagnosis may be challenging and require additional immunohistochemical and molecular tools [15, 62-64]. Recently, our group tested PRAME in MM-H&N and found that it could be very useful for differentiating malignant from benign melanocytic lesions in H&N (especially in small biopsies, highly fragmented and/or necrotic specimens, and for evaluating resection margins) [62-63]. We found that the best-performing cutoff of PRAME-positive cells was that proposed by *Raghavan SS et al* (<60%/≥60%), with 100% and 77.8% of specificity and sensitivity, respectively [63, 64]. In addition, our study showed that: a) high PRAME expression (≥60%) was associated with specific sites (NC/NS/T, nasopharynx, and maxillary sinus), nodular histotype, and female sex; b) PRAME-negative MM-H&N was mainly located in the palate; however, other authors found that PRAME could be a reliable tool for the diagnosis of oral cavity MM-H&N, and future studies are needed to investigate this issue in larger case series [32, 63, 65-67]. Molecular biology techniques (FISH and NGS) are rarely required for the diagnosis of MM-H&N and are mainly used for prognostic-therapeutic stratification [15-32]. However, they could be used to clarify the metastatic and/or primary nature of a malignant melanocytic lesion in H&N. Specifically, a UV-induced molecular profile (*BRAF p.V600E* and *TERTp* mutations) strongly supports the metastatic nature and primary cutaneous origin, whereas *NRAS* and *KIT* mutations favor a primary H&N nature [15-32]. However, molecular results should always be integrated with clinicopathologic and radiologic features for a definitive diagnosis [15-32].

2.5 Prognosis

The prognosis of MM-H&N is poor (5y-S less than 35%), mainly due to local recurrence and/or residual tumor, lymph-node, and distant metastases [47-49, 53-59]. Recent reviews indicated that

local and distant failures are detected to occur in up to 80-85% of patients, regardless of the radicality of surgery and adjuvant therapies [47-49, 53-59]. pT4 stage, infiltration of specific anatomic structures (carotid, cranial nerves, and skull base), positive surgical margins, lympho-vascular invasion, and metastases (lymph-node and distant) are associated with poorer prognosis [47-49, 53-59].

2.6 Staging

In the latest American Joint Committee on Cancer (AJCC) Cancer Staging Manual (8th edition, 2017), the pT stage of MM-H&N comprises pT3 (tumor limited to the mucosa and immediately underlying soft tissue, regardless of thickness or greatest dimension) and pT4 [pT4a: infiltration of deep soft tissue, cartilage, bone, or overlying skin; pT4b: infiltration of the brain, dura, skull base, lower cranial nerves (IX, X, XI, XII), masticator space, carotid artery, pre-vertebral space, or mediastinal structures] stages, regardless of the primary site and omitting pTis/pT1/pT2 to reflect the poor survival also in “superficial” tumors [68]. pN and pM stages are classified as follows: a) NX (regional lymph-nodes cannot be assessed), N0 (no regional-lymph node metastases), and N1 (regional lymph-node metastases present); M0 (no distant metastases), and M1 (distant metastases present) [68]. Notably, pT, pN, and pM stages are not grouped to obtain AJCC prognostic stage groups able to predict survival as for other tumors [68]. Several authors argued that AJCC staging is not effective in predicting prognosis in MM-H&N, and proposed to include the primary site and other clinicopathologic features for subclassification of the the pT stage [68-70]. In addition, future studies are needed to investigate the AJCC staging for rare pharyngeal and laryngeal MM-H&N and

to validate the potential role of nomograms incorporating multiple and independent risk predictors of survival [68-70].

2.7 Therapy

2.7.1 Therapy: surgery

Surgery is the gold standard for the treatment of MM-H&N, but the surgical approach must be individually tailored according to the site, AJCC stage, and infiltration of specific anatomic structures [46-49, 71, 72]. In a significant percentage of patients, especially those with advanced-stage disease, complete surgical resection may not be possible or possible with very minimal surgical margins [46-49, 71, 72]. Consequently, local recurrence and/or residual tumor are common and warrant surgical procedures focused on local disease control and reduction of metastatic risk [46-49, 71, 72]. Failure of local disease control is associated with an increased risk of metastasis and decreased survival (patients with local recurrence and/or residual tumor have a 21-fold increased risk of death of disease) [47-49]. For patients with local recurrence and/or residual tumor, surgery is still considered the best option, but could not be performed in all patients due to frequent infiltration of relevant anatomical structures and the high morbidity of surgical procedures [46-49]. In addition, patients who achieve local disease control after surgery and/or adjuvant radiotherapy often develop lymph-node and/or distant metastases [47-49]. Minimally-invasive endoscopic approaches have recently been proposed as a valid alternative for local disease control, but they need to be validated with long-term follow-up, and at the current state-of-the-art, conventional surgery remains the gold standard [46-49, 71, 72]. Elective treatment of the neck is usually not

performed due to the relatively low incidence of lymph-node metastases at onset (NC/NS/T: 6%, oral cavity: 25%) [46-49]. However, the incidence of lymph-node metastases increases significantly during the course of the disease (NC/NS/T: 20%, oral cavity: 42%), which often justifies surgical removal of the lymph-nodes at a later stage [46-49]. The risk of lymph-node metastasis has been correlated with certain clinicopathologic features (oral cavity, diameter > 4 cm, nodular histotype, and depth of invasion > 5 mm), and some authors have suggested prophylactic neck dissection only in these patients, and close follow-up or sentinel lymph-node biopsy in the others [47-49, 53-59].

2.7.2 Therapy: radiotherapy

Recent meta-analyses have shown that radiotherapy as definitive treatment has a lower 5y-S compared to surgery alone [73-75]. New radiotherapy modalities (carbon-ion, neutron and proton radiotherapy) showed comparable efficacy and lower toxicity than conventional surgery, but need to be further investigated in larger case series [76]. In clinical practice, radiotherapy is mainly adopted in two scenarios: a) adjuvant therapy for advanced-stage MM-H&N, local recurrence and/or residual tumor, and high risk of lymph node involvement according to NCCN guidelines (recommendation on a type 3 basis); b) definitive treatment for unresectable MM-H&N and patients who refuse surgery (recommendation on a type 3 basis) [46]. It should be noted that adjuvant radiotherapy significantly improves the local disease control but not the OS, which has been attributed to the high risk of systemic relapse (lymph-node and distant metastases) [46, 73-76]. Finally, radiotherapy could be adopted for local recurrence and/or residual tumor in combination or not with surgery (recommendation on a type R basis) and as a palliative strategy for metastatic disease (recommendation on a type R basis) [46].

2.7.3 Therapy: systemic therapy

2.7.3.1 Therapy: systemic therapy-chemotherapy and interferon

Dacarbazine chemotherapy has historically been the standard of care for metastatic melanoma, despite a lack of survival benefit and poor response rates [46, 77]. The role of chemotherapy has diminished with the advent of ICIs and is now rarely adopted [46, 77]. Interferon (IFN) is recommended for the adjuvant treatment of cutaneous melanoma (based on type 1 evidence as an individualized option) with improvements in both RFS and OS [46, 78]. However, a phase II trial showed that IFN is less effective than chemotherapy as adjuvant therapy in MM, suggesting that alternative adjuvant approaches should be adopted in this subset of melanoma [46, 79].

2.7.3.2 Therapy: systemic therapy-targeted therapy

MM-H&N has different rates of *BRAF*, *NRAS*, and *KIT* mutations than cutaneous melanoma, justifying a different response to BRAF-inhibitors (dabrafenib, vemurafenib, etc.) alone or in combination with MEK-inhibitors (mekinist, binimetinib, etc.) [26, 46, 80-82]. Due to the relatively high frequency of *NRAS* mutations in NC/NS/T MM-H&N, MEK-inhibitors could be promising drugs for this tumor [26, 46, 81, 82]. Binimetinib was the first agent adopted for *NRAS*-mutated melanoma, with clear evidence that combinations of BRAF- and MEK-inhibitors lead to improved clinical outcomes in both *NRAS*- and *BRAF*-mutated melanoma [46-49, 82]. Oral cavity MM-H&N showed *KIT* mutations in up to 40% of cases, providing a rationale for the use of KIT-inhibitors (imatinib, dasatinib, etc.) in this subset of melanoma [26, 46, 80]. However, a recent meta-analysis

comparing four KIT-inhibitors in patients with advanced-stage MM showed low response rates and high toxicity, suggesting that KIT-inhibitors should be adopted in combination with other agents in MM [80]. *Sheng X et al.* recently combined axitinib (VEGF inhibitor) and ICIs in patients with metastatic MM and found benefits in RFS and OS [83]. It should be emphasized that MM (and MM-H&N) has been excluded from the majority of past and ongoing trials on targeted therapies and ICIs in melanoma (mucosal site is often an exclusion criterion in these trials), with results obtained in cutaneous melanoma being *bona fide* translated to MM [46-49]. This is the major limitation of MM therapy, but recent and ongoing trials focused on MM will be able to provide more reliable results than isolated case reports and small and heterogeneous (cutaneous melanoma and MM) case series [46-49, 83].

2.7.3.3 Therapy: systemic therapy-immunotherapy

Since 2011, when a phase III trial showed that ipilimumab [anti-cytotoxic T-lymphocyte antigen 4 (anti-CTLA-4)] in combination with dacarbazine improved OS compared to dacarbazine alone, ICIs have radically changed the therapy of advanced-stage, unresectable and metastatic melanoma [84]. Although clinical trials focused on MM (and MM-H&N) have been hindered by its rarity, the data on the efficacy and safety of ICIs for MM are growing [46, 85-89]. Three ICIs are approved in Australia and the USA for the treatment of unresectable and metastatic MM: ipilimumab, nivolumab, and pembrolizumab [46]. The analysis of five clinical trials [CA209-003, CA209-038, CheckMate066, CheckMate037, CheckMate067] showed longer RFS and OS with the combination of nivolumab and ipilimumab compared to nivolumab and/or ipilimumab alone in MM [85-89]. Furthermore, several factors complicate the adoption of combined ICIs (higher incidence of grade 3

and 4 treatment-related adverse events, higher incidence of discontinuation, and lower efficacy compared to cutaneous melanoma) in current clinical practice [46-49]. In addition, other studies did not find any benefit of combining ICIs, and future studies are needed to establish the real impact of combined ICIs for unresectable and metastatic MM and MM-H&N [46-49]. Although randomized trials demonstrated improved survival with adjuvant targeted therapy and ICIs in cutaneous melanoma, there is no evidence to conclude that adjuvant therapy (chemotherapy, IFN, targeted therapy, and ICIs) provides any survival benefit for MM and MM-H&N [90]. There is only one randomized trial showing longer OS with an adjuvant combination of temozolomide and cisplatin compared to IFN and observation in MM; moreover, the combination of temozolomide and cisplatin does not improve survival in metastatic MM, and it had been used before the introduction of targeted therapy and ICIs [91]. The ongoing CheckMate238 trial is testing adjuvant nivolumab versus ipilimumab and includes a subcohort of MM (29 patients), but such a small number of patients may preclude useful and informative subgroup analyses, and further studies are needed to test adjuvant ICIs (and other systemic therapies) in MM before their application in clinical practice [46-49, 92]. Neoadjuvant ICIs (a combination of ipilimumab and nivolumab) have shown promising results in advanced-stage cutaneous melanoma, and few preliminary data in MM are encouraging [93-95]. In two recent phase II trials, neoadjuvant ICIs in advanced-stage and resectable MM showed good response rates but a high incidence of grade 3 and 4 treatment-related adverse events [94, 95]. All these findings support the future use of neoadjuvant ICIs in MM and encourage several ongoing clinical trials [46-49, 92-95]. Finally, novel combinations of therapeutic agents (radiotherapy and ICIs, anti-VEGF and ICIs, etc.) represent a promising area of research in MM-H&N and are being investigated in recent and ongoing clinical trials [46-49, 83, 94, 96].

3. Thesis outline

MM-H&N is a rare tumor, characterized by a poor prognosis and limited availability of therapeutic strategies (targeted therapy and ICIs) compared to its cutaneous counterpart [1, 8, 46]. Its rarity, together with the heterogeneity of the case series analyzed (NC/NS/T, oral cavity, both. etc.) and the methods adopted (histology, immunohistochemistry, NGS, FISH, etc.), limits our knowledge and affects the development of innovative therapies [1, 8, 46-49]. Meanwhile, BF-mIHC is emerging as a promising technique for characterizing the TME and has proven to be a valid tool for predicting response to ICIs in several tumors, including melanoma [50-52]. BF-mIHC is a recently introduced technique, and several methodological (visualization systems, scores, chromogen combinations, costs, expertise, etc.) and clinicopathologic (tumors, immune markers, biological and therapeutic implications of the results, etc.) aspects need to be investigated [50-52].

The aims of the present PhD project are:

1. To collect a large and multicenter case series of MM-H&N to describe clinicopathologic features of this melanoma subtype;
2. To analyze the molecular status of MM-H&N and correlate it with clinicopathologic features;
3. To analyze the molecular status of multiple samples obtained from the same patient to verify whether the molecular heterogeneity of MM-H&N could affect the results with relevant implications for the prognostic-therapeutic stratification of these patients;
4. To test a feasible, “easy-to-apply” and reproducible BF-mIHC protocol to study TME in MM-H&N and to be a starting point for future implementations with more complex methodologies (additional chromogens, fusion of two chromogens to obtain "third colors", visualization and

scoring with digital-image analysis);

5. To analyze the correlation between immune markers (CD20, CD3, and CD68) and immune profiles (combination of immune markers) with clinicopathologic and molecular features of MM-H&N to test whether BF-mIHC could be a promising tool for prognostic-therapeutic characterization of these patients;

4. Materials and methods

4.1 Case series

All MM-H&N specimens excised between January 1st 2019 and December 31st 2022 were retrieved from the database of 3 pathology departments located in Bologna (Italy): Bellaria Hospital of Bologna (19), Maggiore Hospital of Bologna (9), and IRCCS Azienda Ospedaliero-Universitaria Policlinico di Sant'Orsola, Bologna (10). Patients were selected according to the following inclusion criteria: (1) primary MM-H&N (each case was reviewed to verify its site and exclude metastases and cases more appropriately classified as cutaneous, especially for the lips); (2) availability of formalin-fixed and paraffin-embedded (FFPE) samples with sufficient material to perform NGS and BF-mIHC analyses; (3) availability of clinical data. In contrast, cases judged to be non-primary mucosal, with no availability of FFPE samples for NGS and BF-mIHC analyses and/or clinical data were excluded. This cohort has been previously published by our group in a study focused on the immunohistochemistry for PRAME in MM-H&N [63]. For each patient, the following clinical data were recorded: age at first diagnosis and sex. For each specimen, the following pathologic features were recorded: type of histologic specimen (excision of primary tumor, excision of local recurrence and/or residual tumor, incisional biopsy), site, histologic subtype, pigmentation, cytotype, ulceration, infiltration of anatomic structures relevant for pT4a stage (deep soft tissues, cartilage, bone, and overlying skin), infiltration of anatomic structures relevant for pT4b stage [brain, dura, skull base, lower cranial nerves (IX, X, XI, XII), masticator space, carotid artery, pre-vertebral space, and mediastinal structures], number of mitoses/mm^2, lympho-vascular invasion (LVI), perineural infiltration (PNI), and pT stage. All cases were

reviewed by a panel of four pathologists with specific expertise in melanocytic pathology and/or head and neck pathology (C.R., B.C., T.B., and M.P.F.) and diagnosed and staged according to the latest WHO Classification of Head and Neck Tumours (fifth edition, 2022) and AJCC Cancer Staging Manual (eighth edition, 2017) [15, 68].

4.2 Molecular analysis

Two 10-µm thick sections were used for DNA extraction using the "QuickExtract™ FFPE DNA Extraction Solution" kit (Lucigen Corporation, Middleton, WI, USA) and quantified using the Qubit dsDNA BR Assay Kit (Thermo Fisher Scientific, Waltham, MA, USA). DNA extraction was performed under microscopic guidance from the representative tumor areas, identified by a pathologist (C.R.) on H&E slides. About 30 ng of DNA was used for amplicons preparation, and sequencing was performed using a laboratory-developed multi-gene NGS panel used at our Solid Tumor Molecular Pathology Laboratory, IRCCS Azienda Ospedaliero-Universitaria di Bologna, University of Bologna Medical Center (Bologna, Italy) for somatic molecular analysis of several solid tumors including CM (330 amplicons total, human reference sequence hg19/GRCh37) [97]. The genomic regions covered by the NGS panel are listed in *Table 1*. To minimize PCR inhibition due to the presence of melanin, 2-3 ul of Betaine 1N was added to the final reaction mix. Templates were then sequenced using an Ion 530 chip, and results were analyzed with Ion Reporter tools v5.18 (Thermo Fisher Scientific). According to previously reported NGS panel validation data, only variants identified in at least 5% of the total number of reads analyzed and observed in both sequencing strands were considered for mutational calls [98]. The Varsome tool

(https://varsome.com/, updated to April 2023) was used to evaluate the American College of Medical Genetics and Genomics (ACMG) classification of each mutation [99].

4.3 BF-mIHC

4.3.1 BF-mIHC: antibodies and chromogens

For each specimen, one representative slide was selected and a 3-µm thick section was cut from the corresponding FFPE tissue block and stained with the following four-label BF-mIHC protocol: CD20, CD3, CD68, and SOX10. The sections were deparaffinized in EZ prep (#950-102; Ventana), and antigen retrieval was achieved by incubation with cell conditioning solution 1 (#950-124; Ventana), a Tris ethylenediaminetetraacetic acid-based buffer (pH 8.2) [51]. Sections were incubated with the following primary antibodies: anti-CD3 (rabbit monoclonal, clone 2GV6, ready-to-use, Ventana Medical System, Tucson, AZ, USA; catalog number: 790-4341), anti-CD20 (mouse monoclonal, clone L26, ready-to-use, Ventana Medical Systems, Tucson, AZ, USA; catalog number: 760-2531), anti-CD68 (mouse monoclonal, clone PGM1, ready-to-use, Diagnostic Biosystems, Pleasanton, CA, USA; catalog number: PDM065), and anti-SOX10 (rabbit monoclonal, clone SP267, ready-to-use, Ventana Medical Systems, Tucson, AZ, USA; catalog number: 760-4968). Each denaturation step was performed by treating the slides with Ultra CC2 (#950-223, ready to use, Ventana Medical Systems, Tucson, AZ, USA) for 8 min. at 100 C° [51]. The signal was developed with anti-mouse or anti-rabbit Alk Phos and anti-mouse or anti-rabbit HRP coupled with the following chromogens: Chromomap DAB (#760-159, ready-to-use, Ventana Medical Systems, Tucson, AZ, USA) for CD3, DISC. PURPLE Kit (#760-229, ready-to-use, Ventana Medical Systems, Tucson, AZ, USA) for CD20, DISC. GREEN HRP Kit (#760-271,

ready-to-use, Ventana Medical Systems, Tucson, AZ, USA) for CD68, DISC. YELLOW Kit (#760-239, ready-to-use, Ventana Medical Systems, Tucson, AZ, USA) for SOX10. The sections were counterstained with Hematoxylin II (#790-2208, ready-to-use, Ventana Medical Systems, Tucson, AZ, USA) [51].

4.3.2 BF-mIHC: methodological considerations

To optimize BF-mIHC procedures and maximize the staining quality in the Ventana Discovery Ultra Immunostainer, we followed a strict methodology for the order of sequential staining, as previously described by *Ugolini F et al*: (1) the antibody with the lowest antigenicity and/or the weakest staining intensity must be the first in the sequence; (2) the sequence must begin with nuclear stains, then cytoplasmic stains, and finally membrane ones; (3) the chromogens combination and order strongly influence the final result, and only chromogens with a translucent nature (Purple, Yellow, and Teal) could be combined in the Ventana Discovery Ultra Immunostainer to target antigens colocalized on the same cell populations and overlap by producing a “third color” [51]. According to *Ugolini F et al*, we performed two different denaturation protocols, combining high temperature and reaction buffer (pH 8.2) or Ultra CC2 (pH 6), both with incubation for 8 min. at 100 °C [51]. Ultra CC2 is a denaturation buffer more efficient than the reaction buffer, ensuring cleaner and brighter colors without altering the previous chromogen staining [51].

4.3.3 BF-mIHC: development and optimization of the protocol

To develop and optimize the four-label BF-mIHC protocol adopted in the current study, we

performed a series of tests with different combinations of chromogens on a subset of 20 cutaneous melanoma samples, as previously described by *Ugolini F et al* [51]. Starting from validated and routinely adopted singleplex staining protocols, we first evaluated whether these protocols could be combined into triple-label BF-mIHC protocols for the detection of immune cells (CD3, CD20, and CD68). We tested three different protocols with the following chromogen combinations: (a) CD3/DAB-CD20/Purple-CD68/Green; (b) CD3/DAB-CD20/Red-CD68/Green; (c) CD3/DAB-CD20/Red-CD68/Purple. The CD3/DAB-CD20/Purple-CD68/Green combination provided the maximum contrast, with the distance of the colors in the visible spectrum making this combination the best-performing choice for the triple-label BF-mIHC protocol (*data not shown*). Since the tested antigens are expressed on the cell membranes of different cells and have similar antigenicity, the order of staining did not affect the final quality of the results [51]. Subsequently, we introduced the nuclear marker SOX10 (highly specific for melanoma cells) and the Yellow chromogen to detect tumor cells and increase the accuracy of immune cells detection and visualization [51]. Again, we tested three combinations, as follows: (a) CD3/DAB-CD20/Purple-CD68/Green-SOX10/Yellow; (b) CD3/Yellow-CD20/Purple-CD68/Green-SOX10/DAB; (c) CD3/Green-CD20/Purple-CD68/Yellow-SOX10/DAB. Since SOX10 is a nuclear marker, we started the sequence with it and then proceeded with the cell membrane markers [51]. We found that the CD3/DAB-CD20/Purple-CD68/Green-SOX10/Yellow combination provided the clearest discrimination between the four stained cell populations (*data not shown*), thus we decided to adopt it. Finally, we tested our subset of 20 cutaneous melanoma samples with singleplex DAB staining for CD20, CD3, CD68, and SOX10 (according to routinely adopted singleplex protocols) to verify the quality and the antigen conservation in the four-label BF-mIHC protocol. We found no differences in nuclear and cell

membrane staining of all the tested antigens between singleplex and four-label BF-mIHC protocols (*data not shown*). These results confirm that our protocol does not cause antigenic loss and/or alteration due to the sequential staining cycles.

4.3.4 BF-mIHC: direct visual interpretation and score system

Slides stained for SOX10 (Yellow), CD3 (Brown), CD20 (Purple), and CD68 (Green) were read on a multi-head microscope by three pathologists, one with specific training in H&N pathology (M.P.F.) and two experienced on TME assessment in different tumors (M.F. and C.R.: previous research publications and national/international meetings on this topic), and agreement was reached for each specimen. We adopted a direct visual interpretation of CD20, CD3, and CD68, which were scored (total number of stained cells) on the hot-spot areas adding up to 1 mm^2, as previously described by us in other tumors [100, 101]. Comparative evaluation of the corresponding H&E slides and SOX10 helped us to correctly assess the immune markers. For patients with multiple specimens, the mean value obtained from the different specimens was used for statistical analyses (*Tables 9*, *10*, and *11*). Finally, we obtained the mean value for CD20, CD3, and CD68 (using all the 38 histologic samples), and each patient has been dichotomized into $CD3_{low}$/$CD3_{high}$, $CD20_{low}$/$CD20_{high}$, and $CD68_{low}$/$CD68_{high}$ based on whether the value was higher or lower than the mean value [100, 101]. In our opinion, due to differences in the microscopes used by different pathologists, the results were more accurately expressed in mm^2 than in high-power fields (HPF) [100, 101].

Two crucial methodological aspects need to be clarified: a) the choice of direct visual interpretation;

b) the identification of hot-spot areas.

a) Direct visual interpretation

The approach for visualizing multiplex staining varies considerably depending on the technique and the primary goal of the analysis [50, 51]. Direct visual interpretation by a pathologist is appropriate for glass slides of low-plex BF-mIHC (as in our study) and digitized slides for mIF, and may be sufficient if used for straightforward tasks, such as tumor immunophenotyping [50, 51]. In contrast, more complex analyses (spatial relationships between cell types) require scanned slides and software for digital-image analysis [50, 51]. Although digital-image analysis provides more accurate results, allows for more complex evaluations, and removes the inter-pathologist variability, it currently has limitations that hinder its adoption [a) suboptimal staining may alter the analysis; b) segmentation is a source of error, potentially misclassifying stroma as cells (and *vice versa*) or fusing and splitting cells; c) compartmentalization may not be perfect (especially if each compartment is not defined by a specific marker); d) exclusion of intercellular stroma by cell-segmentation algorithms; e) poor approximation of cytoplasm in spindled and/or irregularly shaped cells; f) missing of cells with nuclei outside the plane of section; g) high cost; h) complex instrumentation and specific expertise] [50, 51]. Furthermore, although previous studies have shown optimal concordance rates between digital-image analysis and direct visual interpretation, this issue needs to be investigated in future studies focusing on multiplexing [50, 51, 102].

b) Hot-spot areas

In our case series, it was not possible to distinguish between "tumor center" and "invasive margin" compartments, as the majority of specimens were highly fragmented (especially NC/NS/T MM-H&N). For this reason, we decided to adopt a modified version of the state-of-the-art

recommendations of the International Immuno-Oncology Biomarker Working Group for TILs assessment [34-39]. The three compartments potentially used to identify the hot-spot areas were: a) tumoral regions (putatively representing the so-called intra-tumoral tumor center and intra-tumoral invasive margin compartments); b) stromal regions bordered on two sides by tumoral regions [putatively representing the so-called stromal tumor center compartment and the "inner portion" (0-500 µm inside the tumor invasion front) of the stromal invasive margin compartment]; c) stromal regions bordered on only one side by tumoral regions and up to 500 µm away from the tumor invasion front (putatively representing the so-called "outer portion" of the stromal invasive margin compartment) [34-39]. We adopted the definition of "invasive margin" proposed by *Galon J et al*, as "the region centered on the border separating the host tissue from the malignant nests, with an extent of 1 mm" [103]. We excluded necrotic areas, stromal regions bordered on only one side by tumoral regions but more than 500 µm away from the tumor invasion front, stromal regions away from the tumor (the last two potentially representing the so-called stromal peri-tumoral compartment), and specific local tissues such as cartilage, bone, and H&N mucosae [regardless of their localization (infiltrated and intra-tumoral, away from the tumor, and/or at the invasive margin)] [34-39]. As previously mentioned, we counted the total number of CD20, CD3, and CD68 stained cells in the selected hot-spot areas adding up to 1 mm^2, and we obtained a single value for each sample, without distinguishing between the different areas (tumor center vs invasive margin compartments, tumoral vs stromal regions, etc.) [34-39, 100, 101]. Although it is beyond the scope of this PhD project, it should be emphasized that, at the current state-of-the-art, it remains to be clarified whether the whole-slide (as commonly performed with digital-image analysis) is more informative than hot-spot areas (as commonly performed with direct visual interpretation and hot-

spot areas evaluation) for TME assessment and tumor's immune biology (e.g., hot-spot areas evaluation is adopted for several biomarkers in surgical pathology, such as Ki67 in neuroendocrine tumors) [50, 51, 104]. In the present PhD project, we aim to perform a preliminary evaluation of TME in MM-&N with a low-plex four-label (CD20, CD3, CD68, SOX10) BF-mIHC protocol adopting direct visual interpretation and the above-mentioned score ("easy-to-apply" and familiar to pathologists, not requiring complex instrumentation and specific expertise). In the next months, we will add other immune markers (FoxP3, PD-L1, CD163, etc.) to our protocol and compare direct visual interpretation with digital-image analysis.

4.4 Statistical analyses

The clinicopathological features, mutational status, and BF-mIHC results (CD3, CD20, and CD68 scores) were dichotomized and their associations were analyzed using the $\chi 2$ test. Statistical tests were performed using the IBM SPSS software, with a *p-value <0.05* (2-sided) indicating statistical significance.

4.5 Ethical approval

All clinicopathologic investigations were conducted in accordance with the principles of the Declaration of Helsinki and all information regarding the human material used in this study was managed using anonymous numerical codes. The study was approved by the Review Board of the Area Vasta Emilia Centro-AVEC (182/2023/Oss/AOUBo, 202-2022-OSS-AUSLBO-22035, 203-2022-OSS-AUSLBO-22035, EM330-2023-22035-EM1-OSS-AUSLBO, and EM127-2023-22036-EM1-OSS-AUSLBO).

5 Results

5.1 Case Series

A total of 38 histologic specimens were collected from 24 patients: 25 (65.8%) excisions of the primary tumor, 10 (26.3%) excisions of local recurrence/residual tumor, and 3 (7.9%) incisional biopsies, the latter followed by the surgical excision of the primary tumor. Sixteen (66.7%) patients were female and 8 (33.3%) were male; the age at diagnosis ranged from 29 to 96 years (median value: 71 y). The most represented sites were NC/NS/T (27, 71%) and palate (6, 15.8%), followed by maxillary sinus (4, 10.5%) and tongue (1, 2.6%). The most common histologic subtype was nodular (13, 54.2%), with a high percentage of cases showing ulceration (18, 75%) and a predominant epithelioid cytology (14, 58.3%). According to the AJCC (eighth edition, 2017), the pT stages included 18 (75%) pT3, 5 (20.8%) pT4a, and 1 (4.2%) pT4b [68]. The clinicopathologic features of the case series are listed in *Tables 2*, *3*, and *4*, and summarized in *Table 5*. A graphical representation of the clinicopathologic features is shown in *Figures 1* and *2*.

5.2 Molecular analyses

All 38 samples were analyzed by NGS. Four samples (4/38, 10.5%) were not evaluable due to low-quality DNA. Of the remaining 34 samples, 3/34 (8.8%) harbored *TP53* mutations, 3/34 (8.8%) *NRAS* mutations, 3/34 (8.8%) *KIT* mutations, 2/34 (5.9%) *KRAS* mutations, 2/34 (5.9%) *GNAQ* mutations, 1/34 (2.9%) *GNA11* mutation, 1/34 (2.9%) *CTNNB1* mutation, 1/34 (2.9%) *IDH1*

mutation, and 1/34 (2.9%) *BRAF* mutation (*p.N581I* and not *p.V600E*), with only 1/34 (2.9%) specimen showing two different mutated genes: *NRAS* and *EIF1AX*; there were 17/34 (50%) cases with a WT status. The molecular results of the case series are listed in *Table 6* and summarized in *Table 7*. A graphical representation of the molecular results is shown in *Figure 3*. For statistical analyses, the molecular results found in different specimens of the same patient were grouped. The cases were dichotomized as follows: WT and mutated (at least 1 mutation) cases, *BRAF*/*RAS*-mutated and *BRAF*/*RAS*-not-mutated cases, multi-mutated (at least 2 different mutated genes) not-multi-mutated cases; given the results obtained in *BRAF*/*RAS*-mutated cases, we decided to also examine *NRAS*-mutated and *NRAS*-not-mutated cases. The only significant association was found between *BRAF/RAS*-mutated status and the mucosal lentiginous histologic subtype (*p=0.013*); no statistically significant associations were found between molecular status and the other clinicopathologic features. The association between clinicopathologic features and molecular status is summarized in *Table 8* and *Supplementary Material 1*. Among 8 patients with multiple histological specimens and at least two ones evaluable for NGS analysis, 4 (50%) showed divergent molecular results between different specimens: patient #1 (specimen #1: *KRAS*; specimen #2: *TP53*), patient #12 (specimens #17, #20, and #21: WT; specimen #18: *GNA11*; specimen #19: *NRAS*), patient #21 (specimen #33: *BRAF*; specimen #34: WT), patient #24 (specimen #37: WT; specimen #38: *KIT*) (*Table 7*). A graphical representation of the molecular results in patients with multiple specimens and at least two ones evaluable for NGS analysis is shown in *Figure 4*.

5.3 BF-mIHC

The BF-mIHC analyses and the dichotomization of the obtained results showed: a) CD3-mean

value = 443.3/mm^2 [$CD3_{low}$ = 14/24 (58.3%); $CD3_{high}$ = 10/24 (41.7%)]; b) CD20-mean value = 128/mm^2 [$CD20_{low}$ = 14/24 (58.3%); $CD20_{high}$ = 10/24 (41.7%)]; c) CD68-mean value = 212.3/mm^2 [$CD68_{low}$ = 11/24 (58.3%); $CD68_{high}$ = 13/24 (41.7%)]. BF-mIHC results are listed in *Tables 9*, *10*, and *11*. $CD20_{high}$ was significantly associated with LVI [7/9 (77.8%) cases with LVI showed $CD20_{high}$, *p=0.005*] and fused/mixed cytotype [7/10 (70%) cases with fused/mixed cytotype showed $CD20_{high}$, *p=0.017*]. $CD68_{high}$ was significantly associated with advanced pT stage [6/6 (100%) cases with pT4a/pT4b showed $CD68_{high}$, *p=0.009*] and fused/mixed cytotype [8/10 (80%) cases with fused/mixed cytotype showed $CD68_{high}$, *p=0.032*]. Conversely, $CD3_{high}$ was significantly associated with localized pT stage [0/6 (0%) cases with pT4a/pT4b showed $CD3_{high}$, *p=0.017*]. Moreover, $CD3_{high}$ was significantly associated with *BRAF/RAS*-mutated status [5/6 (83.3%) *BRAF/RAS*-mutated cases showed $CD3_{high}$, *p=0.013*], multi-mutated status [3/3 (100%) multi-mutated cases showed $CD3_{high}$, *p=0.025*], and *NRAS*-mutated status [3/3 (100%) *NRAS*-mutated cases showed $CD3_{high}$, *p=0.025*]. The association between BF-mIHC results, clinicopathologic features, and molecular status is summarized in *Table 12*. Illustrative examples of MM-H&N with H&E and BF-mIHC slides are shown in *Figure 5* and *6*.

6 Discussion

MM-H&N has a worse prognosis and fewer therapeutic strategies than its cutaneous counterpart [46-49]. This could be explained by its anatomical (frequent infiltration of relevant anatomical structures) and molecular (lower frequency of molecular alterations treatable with targeted therapy) features, but its rarity limits the collection of large case series and the development of new and effective therapies [46-49]. As a result, MM-H&N is being treated with data obtained in trials on

cutaneous melanoma, even though the mucosal site was paradoxically an exclusion criterion in these trials [46-49]. Meanwhile, BF-mIHC is emerging as a promising technique to characterize TME and predict response to ICIs in several tumors, but many aspects (clinicopathologic, technical, and logistic) of this new tool need to be further clarified [50-52]. In this PhD project, we collected a multi-instiutional case series of MM-H&N, which we analyzed using our laboratory-developed NGS panel and low-plex four-label (CD20, CD3, and CD68) BF-mIHC protocol (direct visual interpretation and scoring system previously adopted by our group) [100, 101].

According to the majority of previous literature, our data confirm: a) relevant involvement of *BRAF*/*RAS* (especially *RAS*) and *KIT* mutations in MM-H&N; b) high number of potentially involved genes (*NRAS*, *KRAS*, *BRAF*, *KIT*, *TP53*, *GNAQ*, *GNA11*, *EIF1AX*, *IDH1*, and *CTNNB1*) in MM-H&N; c) absence of UV-signature (no C>T transitions; no *BRAF p.V600E* and *TERTp* mutations; rare "non-canonical and non-UV-induced" *BRAF* mutations) in MM-H&N; d) a significant percentage of WT cases compared to its cutaneous counterpart [15-33]. Interestingly, recent studies adopting in-depth molecular analyses (targeted and whole DNA- and RNA-NGS panels, large gene NGS panels, PCR, FISH, and Sanger sequencing) found that WT cases may be much lower, with a significant number of cases harboring mutations less known to be involved in the pathogenesis of MM-H&N ("non-canonical") [25-28, 32]. However, these techniques are expensive and are rarely used for routine melanoma characterization in most hospitals and academic institutions [25-28, 32]. In addition, the clinical and prognostic-therapeutic implications of these "non-canonical" mutations in melanoma need to be further investigated [25-28, 32].

We found a statistically significant association between *BRAF*/*RAS* mutations and lentiginous mucosal histotype (*p=0.013*). This finding suggests that there may be an association between mutational signatures and specific histotypes in MM-H&N, as is well-known for cutaneous melanoma [33]. Curiously, no previous studies have investigated the association between molecular status and histology in MM-H&N [15-32].

We did not find a statistically significant association between *BRAF*/*RAS* or *NRAS* mutations and NC/NS/T (*p=0.143*), but these mutations were more frequently found in NC/NS/T [3/6 (50%) *BRAF*/*NRAS* and 2/3 (66.7%) *NRAS* mutations in NC/NS/T] than in oral cavity [2/6 (33%) *BRAF*/*NRAS* and 0/3 (0%) *NRAS* mutations in oral cavity] MM-H&N. These results are consistent with the presumed dominant role of *NRAS* and *BRAF*/*RAS* in the oncogenesis of sino-nasal MM-H&N, as previously described [16, 17, 19, 21, 24, 25, 30, 32]. However, it should be noted that other studies did not find this "molecular status-site" correlation, probably due to the heterogeneity of case series and molecular testing, the combination of cases from NC/NS/T and oral cavity into a single “H&N category”, and the criteria used to define sino-nasal MM-H&N [18, 20, 22, 27-29]. We separated NC/NS/T and maxillary sinus because they are reported as different t in the AJCC (eighth edition, 2017) topography codes list, but in most previous studies NC/NS/T, paranasal sinuses, and nasopharynx are grouped into a single “sino-nasal category” [15-32, 68]. In our case series, 4/6 (66.7%) *BRAF*/*RAS* and 3/3 (100%) *NRAS* mutations were detected in NC/NS/T and maxillary sinus, again emphasizing the predominant role of *BRAF*/*RAS* and *NRAS* signatures in the so-called “sino-nasal” MM-H&N.

One of the most relevant findings of our study is that half of the patients (4/8, 50%) with multiple histological specimens (excision of the primary tumor, excision of local recurrence/residual tumor, and incisional biopsy) and at least two ones evaluable for NGS analysis show divergent molecular results between the different specimens (*Figure 4*). Local recurrences/residual tumors are frequent in MM-H&N, and it is common in clinical practice to have patients with multiple histologic specimens of the same neoplasm [47-49, 53-59]. In contrast, this scenario is much rarer in cutaneous melanoma, except that for the intra-epithelial/superficial component of lentigo maligna melanoma, desmoplastic melanoma, and/or other melanomas occurring at sites not amenable to demolitive surgery (H&N cutaneous melanomas, especially periocular tumors) [33]. Moreover, in these scenarios, local recurrence/residual tumor mainly imply local disease control and/or aesthetic issues (especially in case of multiple surgical procedures), whereas in MM-H&N they are associated with increased risk of metastasis, decreased survival, and deterioration of patient's clinical condition [33, 47-49, 53-59]. Our results suggest that in patients with multiple histologic specimens, NGS analysis of each specimen may be necessary for accurate molecular characterization and prognostic-therapeutic stratification, especially for the potential detection of targetable molecular alterations. Although the pathogenetic basis of this result is beyond the scope of this PhD project and requires specific investigation, it is likely that the “molecular heterogeneity” of MM-H&N may be the answer [105-107]. Notably, the clinical-anamnestic review of these patients showed that none of them underwent adjuvant therapy after surgery (radiotherapy, chemotherapy, IFN, ICIs), suggesting that this result was intrinsic to MM-H&N and not related to the effect of specific therapies.

In recent years, enormous efforts have been made to clarify the pathological and prognostic-therapeutic implications of TME in melanoma [33-46]. However, the methods to study TME and its impact on prognosis and selection of patients to be treated with ICIs still need to be clarified, which argues against the routine assessment of TME in melanoma [33-46]. Multiplexing has recently emerged as a promising tool for characterizing the TME and predicting the response of different tumors to ICIs [50-52]. However, since multiplexing is a complex and newly introduced technique, many clinicopathologic and methodologic issues remain to be clarified [50-52]. Herein, we tested a low-plex four-label BF-mIHC protocol to analyze TME in MM-H&N. We are aware that our BF-mIHC protocol (direct visualization interpretation and "easy-to-apply" score) has some weaknesses and may provide less accurate results than digital-image analysis, but our main goals were to obtain preliminary data on TME in MM-H&N and to identify a tool to serve as a starting point for future implementations with more complex methodologies. In addition, it should be noted that digital-image analysis implies several methodological issues (suboptimal staining, segmentation, compartmentalization, poor approximation of cytoplasm, missing cells, high cost, and specific expertise) [50, 51]. We found relevant associations between immune markers and clinicopathologic and molecular features in MM-H&N. Specifically, we found that $CD20_{high}$ was associated with LVI ($p=0.005$) and fused/mixed cytotype ($p=0.017$), $CD68_{high}$ was associated with advanced pT stage ($p=0.009$) and fused/mixed cytotype ($p=0.032$), and $CD3_{high}$ was associated with localized pT stage ($p=0.017$), *BRAF*/*RAS*-mutated status ($p=0.013$), multi-mutated status ($p=0.025$), and *NRAS*-mutated status ($p=0.025$). Combining these data, we obtained two immune profiles associated with divergent clinicopathologic features and histologies in MM-H&N, as follows: a) $CD20_{high}/CD3_{low}/CD68_{high}$ associated with unfavorable clinicopathologic features (LVI and

advanced pT stage) and fused/mixed cytotype; b) *CD20*$_{low}$/*CD3*$_{high}$/*CD68*$_{low}$ associated with favorable clinicopathologic features (no LVI and localized pT stage) and epithelioid cytotype. In addition, our data suggest that molecular signatures, probably in cooperation with other mechanisms, may influence the immune profile of MM-H&N, as follows: *BRAF*/*RAS*-mutations, multi-mutations, and *NRAS*-mutations may induce CD3 enrichment. Although it is difficult to compare our results with the literature (a large amount of data, heterogeneous and different case series, different techniques for TME analysis, different melanoma subtypes and immune markers analyzed), our results are in line with those found by *Ledderose S et al* in "sino-nasal" melanoma [42, 43]. Using conventional immunohistochemistry, these authors found that TILs, brisk TILs, and high levels of CD3 and CD8 were associated with lower pT stage, increased OS, RFS, and 5y-S in "sino-nasal" melanoma [42, 43].

Potential limitations of our study include (a) small sample size, (b) lack of a validation cohort for our results, (c) no correlation between direct visual interpretation and digital-image analysis, (d) inter-observer variability in direct visual interpretation and application of our score, (e) exclusion of several immune markers (CD8, FoxP3, PD-L1, etc.) relevant for melanoma biology, (f) no follow-up and survival data, (g) only primary MM-H&N, (h) potentially different treatments received by patients in the three involved departments.

7 Conclusions

MM-H&N requires markers to improve its prognostic-therapeutic stratification. Our BF-mIHC protocol identifies "immune profiles" that correlate with prognostic features (pT stage and LVI),

histology (predominant cytotype), and specific molecular signatures (*NRAS*, *BRAF*/*RAS*, and multi-mutations). These results suggest that our BF-mIHC protocol may be an additional tool for prognostic-therapeutic stratification and deserves future studies to be validated, implemented with more complex and sophisticated techniques (digital image-analysis and other immune markers), and correlated with survival and response to ICIs. In addition, we found that a significant proportion of patients with multiple specimens showed discordant results between the different specimens. This finding suggests that NGS analysis of all the specimens may be required for the accurate molecular profiling and prognostic-therapeutic stratification of these patients, especially for the potential adoption of targeted therapy.

8 Tables

Gene	RefSeq	Chromosome	Exon(s) / Region(s)
BRAF	NM_004333.6	chr7	11, 15
CTNNB1	NM_001904.4	chr3	3, 7, 8
DICER1	NM_030621.4	chr14	8, 19, 24, 25, 27
DPYD	NM_000110.4	chr1	11, 13, 22, Intron_5-6, Intron_10-11, Intron_13-14
EGFR	NM_005228.5	chr7	18, 19, 20, 21
EIF1AX	NM_001412.4	chrX	1, 2, Intron_5-6
GNA11	NM_002067.5	chr19	4, 5
GNAQ	NM_002072.5	chr9	4, 5
GNAS	NM_000516.7	chr20	8, 9
H3.3A	NM_001379043.1	chr1	1
HRAS	NM_001130442.2	chr11	2, 3, 4
IDH1	NM_005896.4	chr2	4
IDH2	NM_002168.4	chr15	4
KIT	NM_000222.3	chr4	8, 9, 11, 13, 14, 17
KRAS	NM_033360.4	chr12	2, 3, 4
MED12	NM_005120.3	chrX	1, 2
MET	NM_001127500.3	chr7	2, 14
NRAS	NM_002524.5	chr1	2, 3, 4
PDGFRa	NM_006206.6	chr4	12, 14, 18
PIK3CA	NM_006218.4	chr3	8, 10, 21
PTEN	NM_000314.8	chr10	5
RET	NM_020975.6	chr10	5, 8, 10, 11, 13, 14, 15, 16
RNF43	NM_017763.6	chr17	2, 3, 4, 5, 6, 7, 8, 9, 10
SMAD4	NM_005359.6	chr18	2, 3, 4, 5, 6, 7, 8, 9, 10, 11, 12
TERT	NM_198253.3	chr5	promoter (g.1295141-1295471)
TP53	NM_000546.6	chr17	2, 3, 4, 5, 6, 7, 8, 9, 10, 11
TSHR	NM_000369.5	chr14	1, 2, 3, 4, 5, 6, 7, 8, 9, 10
VHL	NM_000551.4	chr3	1, 2, 3

NGS: next-generation sequencing;

ALMA MATER STUDIORUM
UNIVERSITÀ DI BOLOGNA

8.1 Table 1: genomic regions covered by the adopted NGS panel

ALMA MATER STUDIORUM
UNIVERSITÀ DI BOLOGNA

Patient number	Specimen number	Sex	Age (years)	Type of histological specimen	Site
1	1	M	68	EPT	NC/NS/T
	2			ELR/RT	NC/NS/T
2	3	M	85	IB	NC/NS/T
	4			EPT	NC/NS/T
3	5	F	84	EPT	NC/NS/T
4	6	F	88	EPT	NC/NS/T
5	7	F	58	EPT	NC/NS/T
	8			ELR/RT	NC/NS/T
	9			ELR/RT	NC/NS/T
	10			ELR/RT	NC/NS/T
6	11	F	81	EPT	NC/NS/T
7	12	F	62	EPT	Maxillary sinus
8	13	M	74	EPT	NC/NS/T
9	14	F	65	EPT	NC/NS/T
10	15	F	96	EPT	NC/NS/T
11	16	M	53	EPT	Palate
12	17	F	86	IB	NC/NS/T
	18			EPT	NC/NS/T
	19			ELR/RT	NC/NS/T
	20			ELR/RT	NC/NS/T
	21			ELR/RT	Maxillary sinus
13	22	F	67	EPT	NC/NS/T
	23			ELR/RT	NC/NS/T
14	24	M	70	EPT	NC/NS/T
15	25	F	84	EPT	NC/NS/T
16	26	F	66	EPT	Maxillary sinus
	27			ELR/RT	Maxillary sinus
17	28	F	69	EPT	Palate
18	29	F	65	EPT	NC/NS/T
19	30	M	57	EPT	NC/NS/T
20	31	M	29	EPT	Palate
	32			EPT	Palate
21	33	M	80	EPT	Palate
	34			ELR/RT	Palate
22	35	F	81	EPT	Tongue
23	36	F	83	EPT	NC/NS/T
24	37	F	56	IB	NC/NS/T
	38			EPT	NC/NS/T

EPT: excision of the primary tumor; ELR/RT: excision of local recurrence/residual tumor, IB: incisional biopsy; NC/NS/T: nasal cavity/nasal septum/turbinates;

8.2 Table 2: clinicopathologic features of the case series-1

ALMA MATER STUDIORUM
UNIVERSITÀ DI BOLOGNA

Patient number	Specimen number	Histologic subtype	Pigmentation	Prevalent cytotype	Ulceration	Mitoses/mm^2	LVI	PNI
1	1	ML	Yes	Fused	Yes	4	Yes	No
	2							
2	3	N	Yes	Epithelioid	Yes	5	No	No
	4							
3	5	ML	Yes	Epithelioid	Yes	2	No	No
4	6	N	No	Mixed	Yes	3	No	No
5	7	N	Yes	Fused	Yes	1	No	No
	8							
	9							
	10							
6	11	N	Yes	Epithelioid	No	4	Yes	No
7	12	ML	No	Epithelioid	Yes	4	No	No
8	13	ML	Yes	Epithelioid	Yes	6	No	No
9	14	N	Yes	Epithelioid	Yes	7	Yes	No
10	15	N	Yes	Epithelioid	Yes	5	No	No
11	16	ML	Yes	Fused	Yes	10	Yes	Yes
12	17	ML	Yes	Epithelioid	Yes	4	No	No
	18							
	19							
	20							
	21							
13	22	N	Yes	Mixed	No	2	No	No
	23							
14	24	N	No	Epithelioid	No	5	Yes	No
15	25	N	Yes	Epithelioid	Yes	8	Yes	Yes
16	26	N	Yes	Fused	Yes	5	Yes	No
	27							
17	28	ML	Yes	Mixed	Yes	4	No	No
18	29	N	No	Epithelioid	Yes	3	No	No
19	30	N	No	Mixed	Yes	9	Yes	No
20	31	ML	Yes	Epithelioid	No	2	No	No
	32							
21	33	ML	No	Fused	Yes	3	Yes	No

	34							
22	35	N	No	Epithelioid	Yes	13	No	No
23	36	ML	Yes	Mixed	No	2	No	No
24	37	ML	Yes	Epithelioid	No	4	No	No
	38							

N: nodular; ML: mucosal lentiginous; LVI: lympho-vascular invasion; PNI: perineural infiltration;

8.3 Table 3: clinicopathologic features of the case series-2

ALMA MATER STUDIORUM
UNIVERSITÀ DI BOLOGNA

Patient number	Specimen Number	Infiltration of anatomical structures relevant for pT4a stage	Infiltration of anatomical structures relevant for pT4b stage	pT stage
1	1	No/NE	No/NE	pT3
	2			
2	3	No/NE	No/NE	pT3
	4			
3	5	No/NE	No/NE	pT3
4	6	No/NE	No/NE	pT3
5	7	No/NE	No/NE	pT3
	8			
	9			
	10			
6	11	No/NE	No/NE	pT3
7	12	No/NE	No/NE	pT3
8	13	No/NE	No/NE	pT3
9	14	No/NE	No/NE	pT3
10	15	No/NE	No/NE	pT3
11	16	Yes	No/NE	pT4a
12	17	No/NE	No/NE	pT3
	18			
	19			
	20			
	21			
13	22	No/NE	No/NE	pT3
	23			
14	24	No/NE	No/NE	pT3
15	25	Yes	Yes	pT4b
16	26	Yes	No/NE	pT4a
	27			
17	28	No/NE	No/NE	pT3
18	29	No/NE	No/NE	pT3
19	30	Yes	No/NE	pT4a
20	31	No/NE	No/NE	pT3
	32			
21	33	Yes	No/NE	pT4a
	34			
22	35	No/NE	No/NE	pT3
23	36	No/NE	No/NE	pT3
24	37	Yes	No/NE	pT4a
	38			

NE: not evaluable;

8.4 Table 4: clinicopathologic features of the case series-3

-Anatomical structures relevant for pT4a stage: deep soft tissues, cartilage, bone, and overlying skin;

-Anatomical structures relevant for pT4b stage: brain, dura, skull base, lower cranial nerves (IX, X, XI, XII), masticator space, carotid artery, pre-vertebral space, and mediastinal structures;

ALMA MATER STUDIORUM
UNIVERSITÀ DI BOLOGNA

		MM-H&N
		Patients (N=24)/Histological samples (N=38); n (%)
Age, median value (range)		71 (29-96)
Sex		
	Male	8 (33.3%)
	Female	16 (66.7%)
Site		
	NC/NS/T	27 (71%)
	Palate	6 (15.8%)
	Maxillary sinus	4 (10.5%)
	Tongue	1 (2.6%)
Type of histological specimen		
	EPT	25 (65.8%)
	ELR/RT	10 (26.3%)
	IB	3 (7.9%)
Histologic subtype		
	ML	11 (45.8%)
	N	13 (54.2%)
Pigmentation		
	Yes	17 (70.8%)
	No	7 (29.2%)
Prevalent cytotype		
	Epithelioid	14 (58.3%)
	Fused	5 (28.8%)
	Mixed	5 (28.8%)
Ulceration		
	Yes	18 (75%)
	No	6 (25%)
Mitoses/mm^2, median value (range)		5 (1-13)
LVI		
	Yes	15 (62.5%)
	No	9 (37.5%)
PNI		
	Yes	2 (8.3%)

	No	22 (91.7%)
Infiltration of anatomical structures relevant for pT4a stage		
	Yes	6 (25%)
	No/NE	18 (75%)
Infiltration of anatomical structures relevant for pT4b stage		
	Yes	1 (4.2%)
	No/NE	23 (95.8%)
pT stage		
	pT3	18 (75%)
	pT4a	5 (20.8%)
	pT4b	1 (4.2%)

MM-H&N: mucosal melanoma of the head and neck region; EPT: excision of the primary tumor; ELR/RT: excision of local recurrence/residual tumor; IB: incisional biopsy; NC/NS/T: nasal cavity/nasal septum/turbinates; N: nodular; ML: mucosal lentiginous; LVI: lympho-vascular invasion; PNI: perineural infiltration; NE: not evaluable;

8.5 Table 5: summary of clinicopathologic features of the case series

-Anatomical structures relevant for pT4a stage: deep soft tissues, cartilage, bone, and overlying skin;

-Anatomical structures relevant for pT4b stage: brain, dura, skull base, lower cranial nerves (IX, X, XI, XII), masticator space, carotid artery, pre-vertebral space, and mediastinal structures;

ALMA MATER STUDIORUM
UNIVERSITÀ DI BOLOGNA

Patient number	Specimen number	NGS results (p.)	NGS results (c.)	VAF (%)	ACMG Significance
1	1	*KRAS* (p.Asp92His)	c.274G>C	34.16	VUS
	2	*TP53* (p.Gly334Trp)	c.1000G>T	32.01	Path
2	3	*TP53* (p.Glu294GlyfsTer2)	c.879_880insGGCT	44.69	Likely Path
	4	*TP53* (p.Glu294GlyfsTer2)	c.879_880insGGCT	51.10	Likely Path
3	5	WT			
4	6	WT			
5	7	WT			
	8	NE			
	9	WT			
	10	WT			
6	11	*NRAS* (p.Gln61Arg)	c.182A>G	50.36	Path
		EIF1AX (p.Arg14Ser)	c.42G>C	42.16	VUS
7	12	*NRAS* (p.Gly12Ala)	c.35G>C	43.63	Path
8	13	NE			
9	14	WT			
10	15	WT			
11	16	WT			
12	17	WT			
	18	*GNA11* (p.Gly188Ser)	c.562G>A	18.75	Likely Path
	19	*NRAS* (p.Gly12Arg)	c.34G>C	25.20	Path
	20	WT			
	21	WT			
13	22	*KIT* (p.Lys642Glu)	c.1924A>G	55.26	Path
	23	*KIT* (p.Lys642Glu)	c.1924A>G	55.26	Path
14	24	WT			
15	25	*CTNNB1* (p.Gly34_His36delinsAsp)	c.101_106delGAATCC	30.10	Path
16	26	*GNAQ* (p.Gln209Pro)	c.626A>C	12.30	Path
	27	*GNAQ* (p.Gln209Pro)	c.626A>C	15.92	Path
17	28	NE			

18	29	*IDH1* (p.Trp124Ter)	c.372G>A	17.27	VUS
19	30	WT			
20	31	*KRAS* (p.Gly12Ser)	c.34G>A	86.85	Path
	32	NE			
21	33	*BRAF* (p.Asn581Ile)	c.1742A>T	23.03	Path
	34	WT			
22	35	WT			
23	36	WT			
24	37	WT			
	38	*KIT* (p.Leu576Pro)	c.1727T>C	51	Path

NGS: next-generations sequencing; VAF: variant allele frequency; ACMG: American College of Medical Genetics and Genomics; Path: pathogenic; Likely Path: likely pathogenic; VUS: variant of unknown significance; WT: wild-type; NE: not evaluable;

8.6 Table 6: molecular results

Gene	Number of histologic specimens with specific mutations, absolute number (%)
KRAS	2/34 (5.9%)
NRAS	3/34 (8.8%)
BRAF	1/34 (2.9%)
EIF1AX	1/34 (2.9%)
TP53	3/34 (8.8%)
GNAQ	2/34 (5.9%)
GNA11	1/34 (2.9%)
KIT	3/34 (8.8%)
CTNNB1	1/34 (2.9%)
IDH1	1/34 (2.9%)
WT	17/34 (50.0%)
NE	4/38 (10.5%)

NGS: next-generations sequencing; WT: wild-type; NE: not evaluable;

8.7 Table 7: summary of the molecular results

The frequency of mutated genes was calculated using the 34 cases with evaluable NGS results (the 4 cases with low-quality DNA and NE results were not counted).

	WT	Mutated		*BRAF/RAS*-mutated	*BRAF/RAS*-not-mutated		Multi-mutated	Not-multi-mutated	
Male	3	4	*p=0.867*	3	4	*p=0.262*	1	6	*p=0.952*
Female	7	8		3	12		2	13	
NC/NS/T	8	8	*p=0.484*	3	13	*p=0.143*	3	13	*p=0.254*
Other sites	2	4		3	3		0	6	
Palate	1	2	*p=0.650*	2	1	*p=0.099*	0	3	*p=0.459*
Other sites	9	10		4	15		3	16	
ML	3	6	*p=0.342*	5	4	*p=0.013*	2	7	*p=0.329*
N	7	6		1	12		1	12	
Epithelioid	5	8	*p=0.429*	4	9	*p=0.658*	2	11	*p=0.774*
Mixed and Fused	5	4		2	7		1	8	
Pigmentation-Yes	6	9	*p=0.452*	4	11	*p=0.926*	3	12	*p=0.203*
Pigmentation-No	4	3		2	5		0	7	
Ulceration-Yes	8	8	*p=0.484*	4	12	*p=0.696*	2	14	*p=0.800*
Ulceration-No	2	4		2	4		1	5	
LVI-Yes	4	5	*p=0.937*	3	6	*p=0.595*	2	7	*p=0.329*
LVI-No	6	7		3	10		1	12	
PNI-Yes	1	1	*p=0.892*	0	2	*p=0.364*	0	2	*p=0.556*
PNI-No	9	11		6	14		3	17	
pT3	8	8	*p=0.484*	5	11	*p=0.494*	3	13	*p=0.254*
pT4a/pT4b	2	4		1	5		0	6	

NGS: next-generations sequencing; NC/NS/T: nasal cavity/nasal septum/turbinates; WT: wild-type; N: nodular; ML: mucosal lentiginous; LVI: lympho-vascular invasion; PNI: perineural infiltration;

8.8 Table 8: association between molecular status and clinicopathologic features

The number of patients included in the statistical analyses was 22, because two patients (*patients #8* and *#17*) did not have specimens with evaluable NGS results.

The molecular status of each individual patient was obtained by summing the NGS results in each specimen collected from that patient.

Patient number	**Specimen number**	**CD20/mm^2**	**CD20-adopted value**	***CD20$_{low}$/ CD20$_{high}$***
1	1	215	196.5	*CD20$_{high}$*
	2	178		
2	3	9	23	*CD20$_{low}$*
	4	37		
3	5	120	120	*CD20$_{low}$*
4	6	165	165	*CD20$_{high}$*
5	7	28	109.8	*CD20$_{low}$*
	8	145		
	9	166		
	10	100		
6	11	19	19	*CD20$_{low}$*
7	12	257	257	*CD20$_{high}$*
8	13	55	55	*CD20$_{low}$*
9	14	170	170	*CD20$_{high}$*
10	15	84	84	*CD20$_{low}$*
11	16	278	278	*CD20$_{high}$*
12	17	126	65.6	*CD20$_{low}$*
	18	41		
	19	137		
	20	14		

	21	10		
13	22	4	13	*CD20$_{low}$*
	23	22		
14	24	292	292	*CD20$_{high}$*
15	25	92	92	*CD20$_{low}$*
16	26	192	203	*CD20$_{high}$*
	27	214		
17	28	122	122	*CD20$_{low}$*
18	29	97	97	*CD20$_{low}$*
19	30	235	235	*CD20$_{high}$*
20	31	27	48	*CD20$_{low}$*
	32	69		
21	33	376	377.5	*CD20$_{high}$*
	34	379		
22	35	83	83	*CD20$_{low}$*
23	36	193	193	*CD20$_{high}$*
24	37	101	56	*CD20$_{low}$*
	38	11		

BF-mIHC: bright-field multiplex immunohistochemistry;

8.9 Table 9: BF-mIHC results for CD20

ALMA MATER STUDIORUM
UNIVERSITÀ DI BOLOGNA

Patient number	Specimen number	CD3/mm^2	CD3-adopted value	$CD3_{low}$/ $CD3_{high}$
1	1	599	566.5	$CD3_{high}$
	2	534		
2	3	195	244	$CD3_{low}$
	4	293		
3	5	340	340	$CD3_{low}$
4	6	1470	1470	$CD3_{high}$
5	7	434	467	$CD3_{high}$
	8	506		
	9	430		
	10	498		
6	11	1315	1315	$CD3_{high}$
7	12	726	726	$CD3_{high}$
8	13	315	315	$CD3_{low}$
9	14	497	497	$CD3_{high}$
10	15	191	191	$CD3_{low}$
11	16	89	89	$CD3_{low}$
12	17	434	620.2	$CD3_{high}$
	18	720		
	19	895		
	20	380		
	21	672		
13	22	251	291	$CD3_{low}$
	23	331		
14	24	739	739	$CD3_{high}$
15	25	152	152	$CD3_{low}$
16	26	205	202	$CD3_{low}$
	27	199		

17	28	524	524	*CD3$_{high}$*
18	29	331	331	*CD3$_{low}$*
19	30	140	140	*CD3$_{low}$*
20	31	820	555	*CD3$_{high}$*
	32	290		
21	33	170	146.5	*CD3$_{low}$*
	34	123		
22	35	395	395	*CD3$_{low}$*
23	36	410	410	*CD3$_{low}$*
24	37	208	115.5	*CD3$_{low}$*
	38	23		

BF-mIHC: bright-field multiplex immunohistochemistry;

8.10 Table 10: BF-mIHC results for CD3

ALMA MATER STUDIORUM
UNIVERSITÀ DI BOLOGNA

Patient number	Specimen number	CD68/mm^2	CD68-adopted value	$CD68_{low}$/ $CD68_{high}$
1	1	224	350	$CD68_{high}$
	2	476		
2	3	94	100.5	$CD68_{low}$
	4	107		
3	5	181	181	$CD68_{low}$
4	6	303	303	$CD68_{high}$
5	7	281	246	$CD68_{high}$
	8	211		
	9	56		
	10	80		
6	11	95	95	$CD68_{low}$
7	12	63	63	$CD68_{low}$
8	13	90	90	$CD68_{low}$
9	14	202	202	$CD68_{low}$
10	15	225	225	$CD68_{high}$
11	16	286	286	$CD68_{high}$
12	17	290	226	$CD68_{high}$
	18	221		
	19	301		
	20	90		
	21	228		
13	22	23	96.5	$CD68_{low}$
	23	170		
14	24	226	226	$CD68_{high}$
15	25	476	476	$CD68_{high}$
16	26	321	317.5	$CD68_{high}$
	27	314		

17	28	86	86	*CD68*$_{low}$
18	29	167	167	*CD68*$_{low}$
19	30	291	291	*CD68*$_{high}$
20	31	40	54	*CD68*$_{low}$
	32	68		
21	33	248	250.5	*CD68*$_{high}$
	34	253		
22	35	181	181	*CD68*$_{low}$
23	36	224	224	*CD68*$_{high}$
24	37	378	437	*CD68*$_{high}$
	38	496		

BF-mIHC: bright-field multiplex immunohistochemistry;

8.11 Table 11: BF-mIHC results for CD68

	CD20$_{low}$	*CD20$_{high}$*		*CD3$_{low}$*	*CD3$_{high}$*		*CD68$_{low}$*	*CD68$_{high}$*	
Male	3	5	*p=0.143*	5	3	*p=0.770*	3	5	*p=0.562*
Female	11	5		9	7		8	8	
NC/NS/T	11	6	*p=0.324*	10	7	*p=0.939*	7	10	*p=0.476*
Other sites	3	4		4	3		4	3	
Palate	2	2	*p=0.711*	2	2	*p=0.711*	2	2	*p=0.855*
Other sites	12	8		12	8		9	11	
ML	6	5	*p=0.729*	6	5	*p=0.729*	5	6	*p=0.973*
Nodular	8	5		8	5		6	7	
Epithelioid	11	3	*p=0.017*	8	6	*p=0.889*	9	5	*p=0.032*
Mixed and Fused	3	7		6	4		2	8	
Pigmentation-Yes	12	5	*p=0.058*	10	7	*p=0.939*	8	9	*p=0.851*
Pigmentation-No	2	5		4	3		3	4	
Ulceration-Yes	10	8	*p=0.633*	11	7	*p=0.633*	8	10	*p=0.813*
Ulceration-No	4	2		3	3		3	3	
LVI-Yes	2	7	*p=0.005*	5	4	*p=0.831*	2	7	*p=0.072*
LVI-No	12	3		9	6		9	6	
PNI-Yes	1	1	*p=0.803*	2	0	*p=0.212*	0	2	*p=0.174*
PNI-No	13	9		12	10		11	11	
pT3	12	6	*p=0.151*	8	10	*p=0.017*	11	7	*p=0.009*
pT4a/pT4b	2	4		6	0		0	6	
WT	4	6	*p=0.211*	6	4	*p=0.937*	3	7	*p=0.342*
Mutated	8	4		7	5		6	6	
***BRAF/RAS*-mutated**	3	3	*p=0.793*	1	5	*p=0.013*	3	3	*p=0.595*
***BRAF/RAS*-not-mutated**	9	7		12	4		6	10	
Multi-mutated	2	1	*p=0.650*	0	3	*p=0.025*	1	2	*p=0.774*
Not-multi-mutated	10	9		13	6		8	11	

NC/NS/T: nasal cavity/nasal septum/turbinates; WT: wild-type; N: nodular; ML: mucosal lentiginous; LVI: lympho-vascular invasion; PNI: perineural infiltration;

8.12 Table 12: association between BF-mIHC results, relevant clinicopathologic features and molecular status

The number of patients included in the statistical analyses was 22, because two patients (*patients #8* and *#17*) did not have specimens with evaluable NGS results.

9. Figures

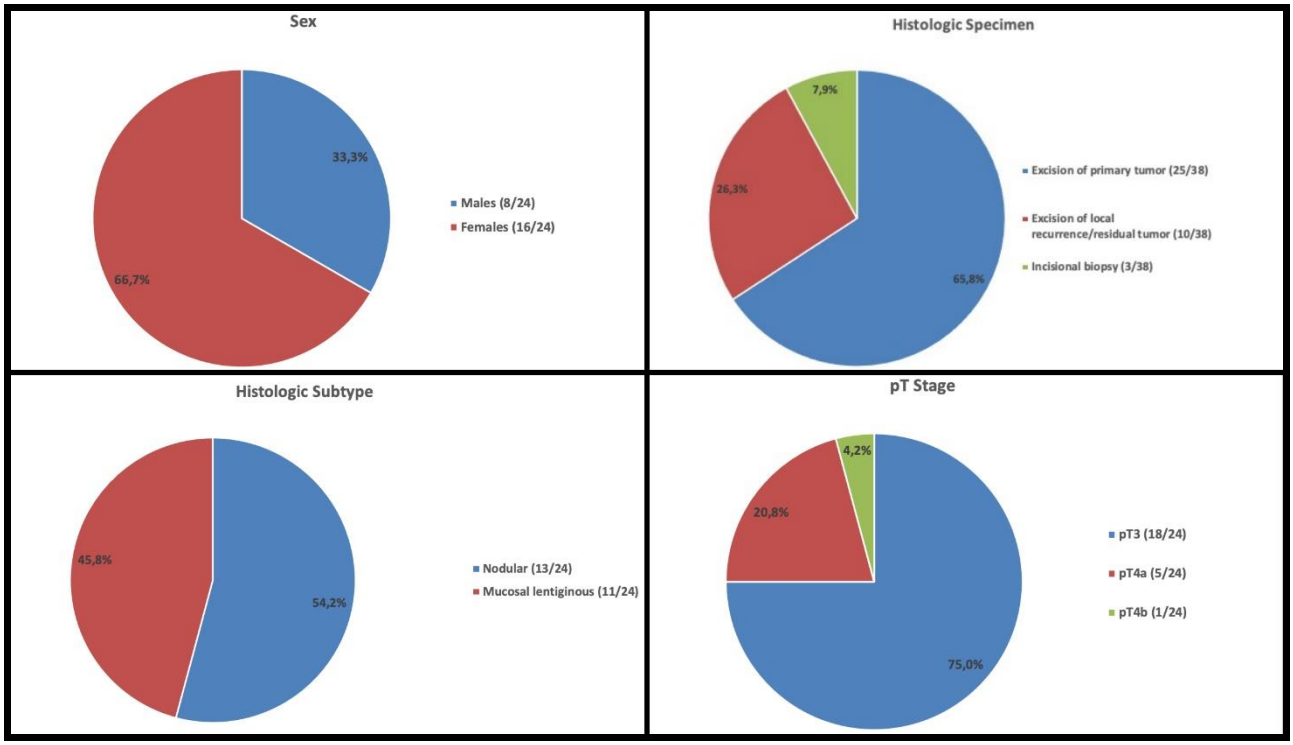

9.1 Figure 1: graphical representation of clinicopathologic features-1

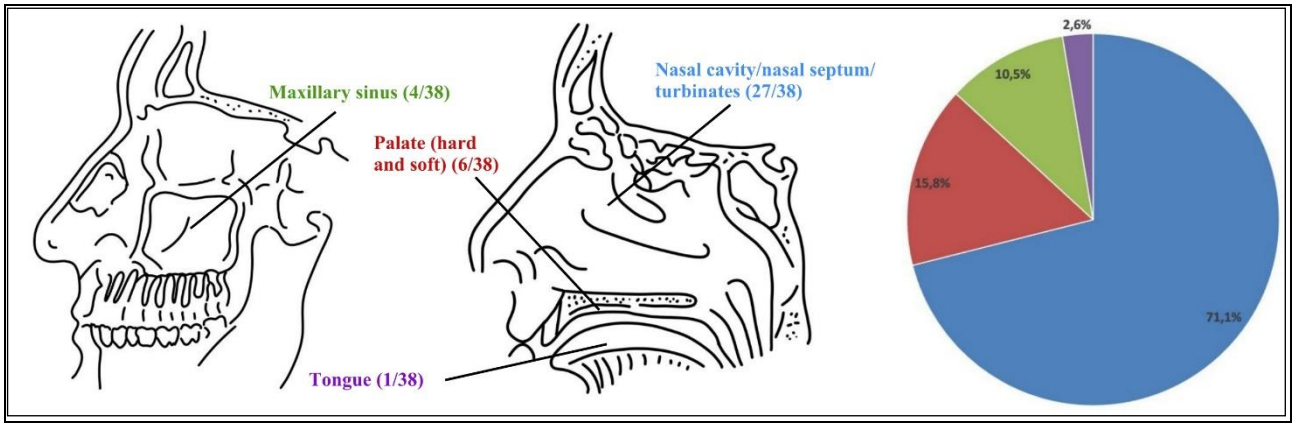

9.2 Figure 2: graphical representation of clinicopathologic features-2

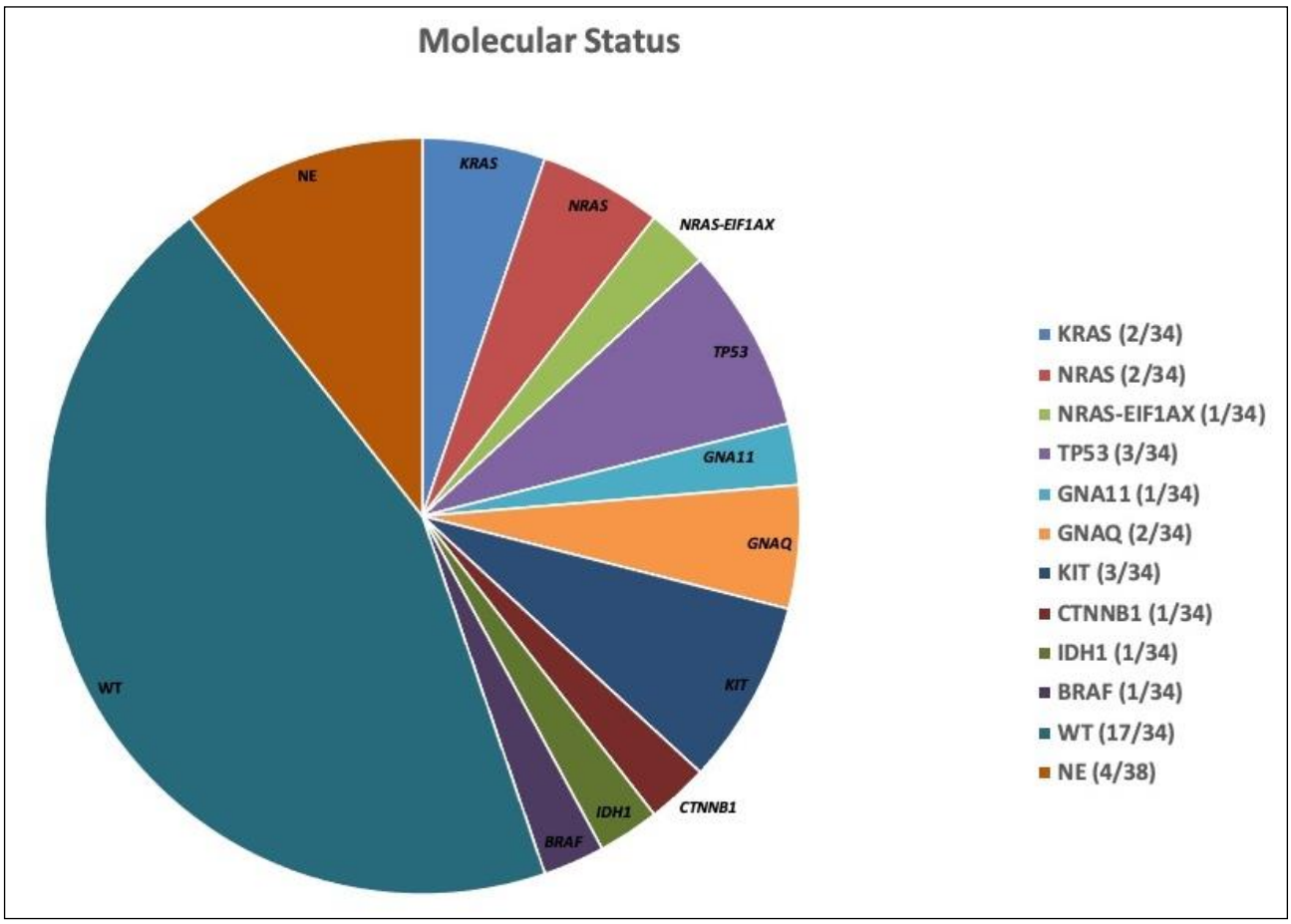

NGS: next-generations sequencing; WT: wild-type; NE: not evaluable;

9.3 Figure 3: graphical representation of the molecular results

On the right, the mutated genes were reported using 34 as the denominator (cases with evaluable NGS results, and the 4 cases with low-quality DNA and NE results were excluded).

In the graph, the mutated genes and the corresponding areas were reported using 38 as the denominator (also the 4 cases with NE results were included).

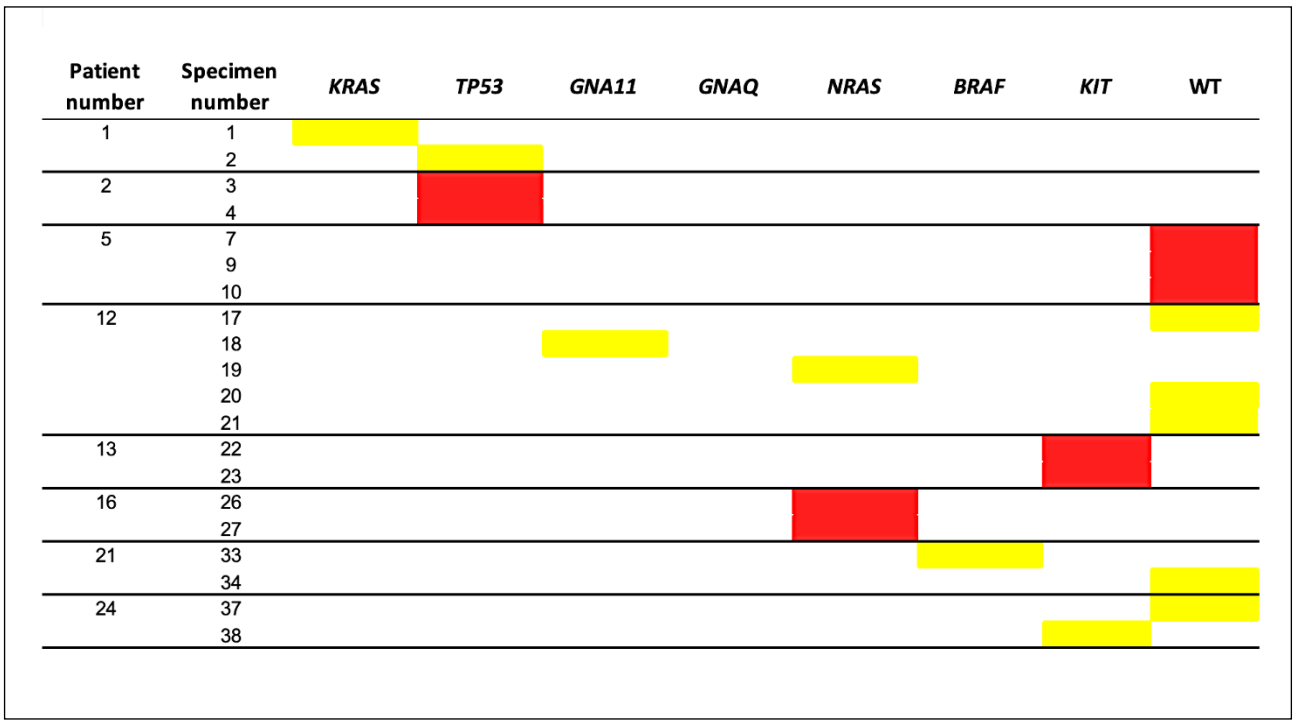

NGS: next-generations sequencing; WT: wild-type;

9.4 Figure 4: graphical representation of molecular results in patients with multiple specimens and at least two ones evaluable for NGS analysis

Yellow squares: patients with discordant molecular results.

Red squares: patients with discordant molecular results.

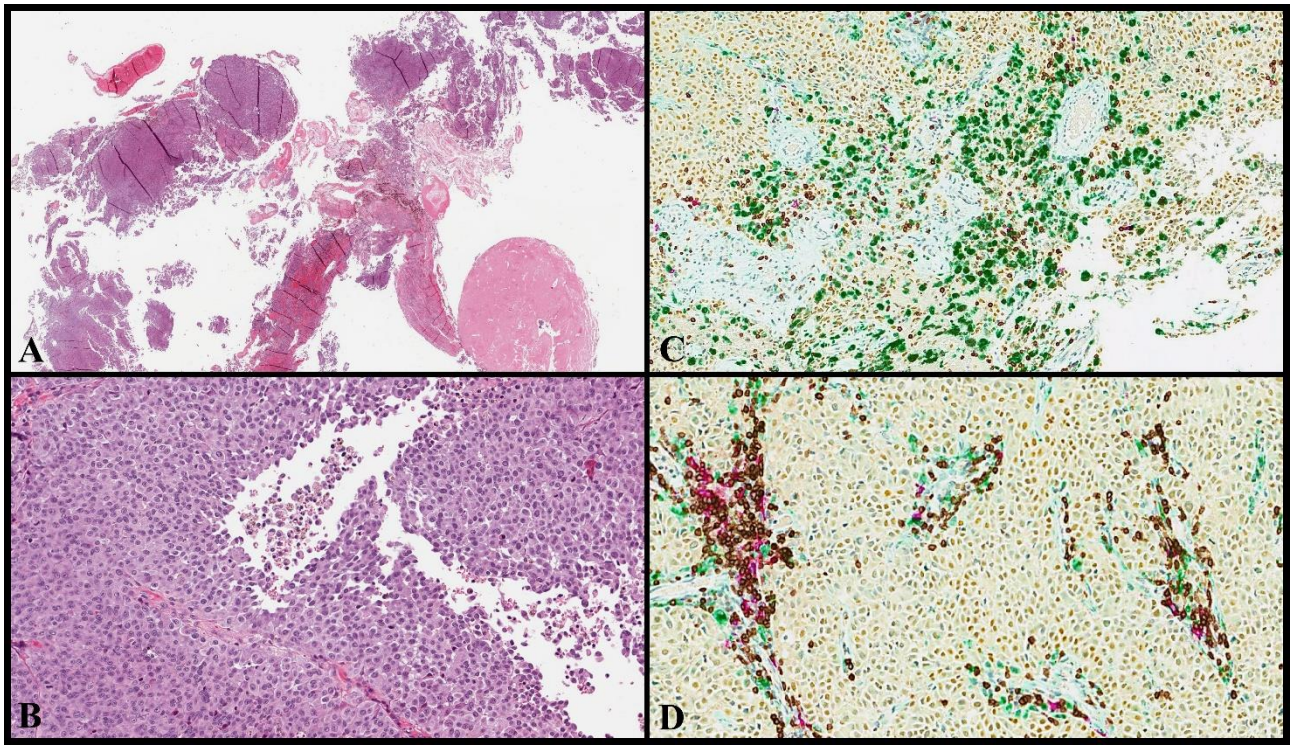

MM-H&N: mucosal melanoma of the head and neck region; BF-mIHC: bright-field multiplex immunohistochemistry; TME: tumor microenvironment; NC/NS/T: nasal cavity/nasal septum/turbinates; H&E: hematoxylin and eosin;

9.5 Figure 5: illustrative example of nodular MM-H&N

A: H&E, original magnification 15x;

B: H&E, original magnification 200x;

C: BF-mIHC [CD20 (Purple), CD3 (DAB-Brown), CD68 (Green), SOX10 (Yellow)], original magnification 150x;

D: BF-mIHC [CD20 (Purple), CD3 (DAB-Brown), CD68 (Green), SOX10 (Yellow)], original magnification 200x;

Highly fragmented specimen of NC/NS/T MM-H&N with a predominant epithelioid cytology (A and B) and two hot-spot areas (C and D) adopted for TME assessment.

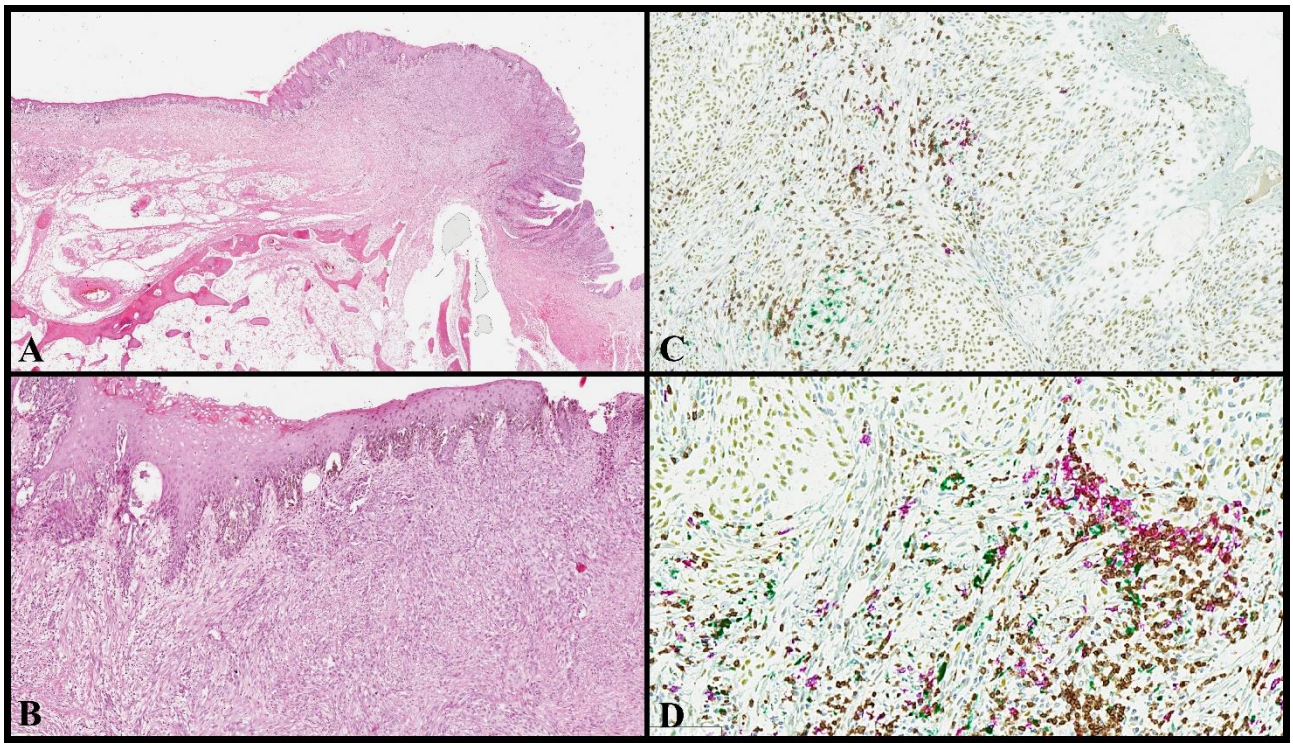

MM-H&N: mucosal melanoma of the head and neck region; BF-mIHC: bright-field multiplex immunohistochemistry; TME: tumor microenvironment; H&E: hematoxylin and eosin;

9.6 Figure 6: illustrative example of lentiginous MM-H&N

A: H&E, original magnification 15x;

B: H&E, original magnification 150x;

C: BF-mIHC [CD20 (Purple), CD3 (DAB-Brown), CD68 (Green), SOX10 (Yellow)], original magnification 150x;

D: BF-mIHC [CD20 (Purple), CD3 (DAB-Brown), CD68 (Green), SOX10 (Yellow)], original magnification 200x;

ALMA MATER STUDIORUM
UNIVERSITÀ DI BOLOGNA

10. Supplementary materials

	***NRAS*-mutated**	***NRAS*-not-mutated**	
Male	0	7	*p=0.203*
Female	3	12	
NC/NS/T	2	14	*p=0.800*
Other sites	1	5	
Palate	0	3	*p=0.459*
Other sites	3	16	
ML	2	7	*p=0.329*
N	1	12	
Epithelioid	3	10	*p=0.121*
Mixed and Fused	0	9	
Pigmentation-Yes	2	13	*p=0.952*
Pigmentation-No	1	6	
Ulceration-Yes	2	14	*p=0.800*
Ulceration-No	1	5	
LVI-Yes	1	8	*p=0.774*
LVI-No	2	11	
PNI-Yes	0	2	*p=0.556*
PNI-No	3	17	
pT3	3	13	*p=0.254*
pT4a/pT4b	0	6	

NGS: next-generation sequencing; NC/NS/T: nasal cavity/nasal septum/turbinates; WT: wild-type; N: nodular; ML: mucosal lentiginous; LVI: lympho-vascular invasion; PNI: perineural infiltration;

ALMA MATER STUDIORUM
UNIVERSITÀ DI BOLOGNA

10.1 Supplementary material 1: association between *NRAS* status and clinicopathologic features

The number of patients included in the statistical analyses was 22, because two patients (*patients #8* and *#17*) did not have specimens with evaluable NGS results.

The molecular status of each individual patient was obtained by summing the NGS results in each specimen collected from that patient.

	CD20$_{low}$	*CD20$_{high}$*		*CD3$_{low}$*	*CD3$_{high}$*		*CD68$_{low}$*	*CD68$_{high}$*	
***NRAS*-mutated**	2	1	*p=0.650*	0	3	*p=0.025*	2	1	*p=0.329*
***NRAS*-not-mutated**	10	9		13	6		7	12	

NGS: next-generation sequencing;

10.2 Supplementary material 2: association between BF-mIHC results and *NRAS* status

The number of patients included in the statistical analyses was 22, because two patients (*patients #8* and *#17*) did not have specimens with evaluable NGS results.

11. References

1. Chang AE, Karnell LH, Menck HR. The National Cancer Data Base report on cutaneous and noncutaneous melanoma: a summary of 84,836 cases from the past decade. The American College of Surgeons Commission on Cancer and the American Cancer Society. *Cancer*. 1998;83:1664-78.

2. Patel SG, Prasad ML, Escrig M, et al. Primary mucosal malignant melanoma of the head and neck. *Head Neck*. 2002;24:247-57.

3. Temmermand D, Kilic S, Mikhael M, et al. Sinonasal Mucosal Melanoma: A Population-based Comparison of the EUROCARE and SEER Registries. *Int Arch Otorhinolaryngol*. 2022;26:e446-52.

4. McLaughlin CC, Wu XC, Jemal A, et al. Incidence of noncutaneous melanomas in the U.S. *Cancer*. 2005;103:1000-7.

5. Youssef D, Vasani S, Marquess J, et al. Rising incidence of head and neck mucosal melanoma in Australia. *J Laryngol Otol*. 2017;131:S25-8.

6. Marcus DM, Marcus RP, Prabhu RS, et al. Rising incidence of mucosal melanoma of the head and neck in the United States. *J Skin Cancer*. 2012;2012:231693.

7. Altieri L, Wong MK, Peng DH, et al. Mucosal melanomas in the racially diverse population of California. *J Am Acad Dermatol*. 2017;76:250-7.

8. Chi Z, Li S, Sheng X, et al. Clinical presentation, histology, and prognoses of malignant melanoma in ethnic Chinese: a study of 522 consecutive cases. *BMC Cancer*. 2011;11:85.

9. Takagi M, Ishikawa G, Mori W. Primary malignant melanoma of the oral cavity in Japan. With special reference to mucosal melanosis. *Cancer*. 1974;34:358-70.

10. Qian Y, Johannet P, Sawyers A, et al. The ongoing racial disparities in melanoma: An analysis of the Surveillance, Epidemiology, and End Results database (1975-2016). *J Am Acad Dermatol*. 2021;84:1585-93.

11. Hicks MJ, Flaitz CM. Oral mucosal melanoma: epidemiology and pathobiology. *Oral Oncol*. 2000;36:152-69.

12. Holmstrom M, Lund VJ. Malignant melanomas of the nasal cavity after occupational exposure to formaldehyde. *Br J Ind Med*. 1991;48:9-11.

13. Lundberg R, Brytting M, Dahlgren L, et al. Human herpes virus DNA is rarely detected in non-UV light-associated primary malignant melanomas of mucous membranes. *Anticancer Res*. 2006;26(5B):3627-31.

14. Gorsky M, Epstein JB. Melanoma arising from the mucosal surfaces of the head and neck. *Oral Surg Oral Med Oral Pathol Oral Radiol Endod*. 1998;86:715-9.

15. WHO Classifications of Tumors Editorial Board. *WHO Classification of Tumours Series: Head and Neck Tumours [Internet; beta version ahead of print]*, 5th ed. International Agency for Research on Cancer; 2022.

16. Chraybi M, Abd Alsamad I, Copie-Bergman C, et al. Oncogene abnormalities in a series of primary melanomas of the sinonasal tract: NRAS mutations and cyclin D1 amplification are more frequent than KIT or BRAF mutations. *Hum Pathol*. 2013;44:1902-11.

17. Öztürk Sari Ş, Yilmaz İ, Taşkin OÇ, et al. BRAF, NRAS, KIT, TERT, GNAQ/GNA11 mutation profile analysis of head and neck mucosal melanomas: a study of 42 cases. *Pathology*. 2017;49:55-61.

18. Toscano de Mendonça UB, Cernea CR, Matos LL, et al. Analysis of KIT gene mutations in patients with melanoma of the head and neck mucosa: a retrospective clinical report. *Oncotarget*. 2018;9:22886-94.

19. Turri-Zanoni M, Medicina D, Lombardi D, et al. Sinonasal mucosal melanoma: Molecular profile and therapeutic implications from a series of 32 cases. *Head Neck*. 2013;35:1066-77.

20. Wroblewska JP, Mull J, Wu CL, et al. SF3B1, NRAS, KIT, and BRAF Mutation; CD117 and cMYC Expression; and Tumoral Pigmentation in Sinonasal Melanomas: An Analysis With Newly Found Molecular Alterations and Some Population-Based Molecular Differences. *Am J Surg Pathol*. 2019;43:168-77.

21. Zebary A, Jangard M, Omholt K, et al. KIT, NRAS and BRAF mutations in sinonasal mucosal melanoma: a study of 56 cases. *Br J Cancer*. 2013;109:559-64.

22. Colombino M, Paliogiannis P, Cossu A, et al. BRAF Mutations and Dysregulation of the MAP Kinase Pathway Associated to Sinonasal Mucosal Melanomas. *J Clin Med*. 2019;8:1577.

23. Ablain J, Xu M, Rothschild H, et al. Human tumor genomics and zebrafish modeling identify SPRED1 loss as a driver of mucosal melanoma. *Science*. 2018;362:1055-60.

24. Amit M, Tam S, Abdelmeguid AS, et al. Mutation status among patients with sinonasal mucosal melanoma and its impact on survival. *Br J Cancer*. 2017;116:1564-71.

25. Freiberger SN, Morand GB, Turko P, et al. Morpho-Molecular Assessment Indicates New Prognostic Aspects and Personalized Therapeutic Options in Sinonasal Melanoma. *Cancers (Basel)*. 2019;11:1329.

26. Hayward NK, Wilmott JS, Waddell N, et al. Whole-genome landscapes of major melanoma subtypes. *Nature*. 2017;545:175-80.

27. Hintzsche JD, Gorden NT, Amato CM, et al. Whole-exome sequencing identifies recurrent SF3B1 R625 mutation and comutation of NF1 and KIT in mucosal melanoma. *Melanoma Res*. 2017;27:189-99.

28. Newell F, Kong Y, Wilmott JS, et al. Whole-genome landscape of mucosal melanoma reveals diverse drivers and therapeutic targets. *Nat Commun*. 2019;10:3163.

29. Chen F, Zhang Q, Wang Y, et al. *KIT*, *NRAS*, *BRAF* and *FMNL2* mutations in oral mucosal melanoma and a systematic review of the literature. *Oncol Lett*. 2018;15:9786-92.

30. Buery RR, Siar CH, Katase N, et al. NRAS and BRAF mutation frequency in primary oral mucosal melanoma. *Oncol Rep*. 2011;26:783-7.

31. Wei D, Chen D, Li L, et al. ALG8-RET: A novel RET rearrangement in a patient with malignant melanoma of the palatal mucosal. *Oral Oncol*. 2020;111:104973.

32. Chłopek M, Lasota J, Thompson LDR, et al. Alterations in key signaling pathways in sinonasal tract melanoma. A molecular genetics and immunohistochemical study of 90 cases and comprehensive review of the literature. *Mod Pathol*. 2022;35:1609-17.

33. WHO Classifications of Tumors Editorial Board. *WHO Classification of Tumours Series: Skin Tumours [Internet; beta version ahead of print]*, 5th ed. International Agency for Research on Cancer; 2023.

34. Salgado R, Denkert C, Demaria S, et al. The evaluation of tumor-infiltrating lymphocytes (TILs) in breast cancer: recommendations by an International TILs Working Group 2014. *Ann Oncol*. 2015;26:259-71.

35. Denkert C, Wienert S, Poterie A, et al. Standardized evaluation of tumor-infiltrating lymphocytes in breast cancer: results of the ring studies of the international immuno-oncology biomarker working group. *Mod Pathol*. 2016;29:1155-64.

36. Amgad M, Stovgaard ES, Balslev E, et al. Report on computational assessment of Tumor Infiltrating Lymphocytes from the International Immuno-Oncology Biomarker Working Group. *NPJ Breast Cancer*. 2020;6:16.

37. Hendry S, Salgado R, Gevaert T, et al. Assessing Tumor-Infiltrating Lymphocytes in Solid Tumors: A Practical Review for Pathologists and Proposal for a Standardized Method from the International Immuno-Oncology Biomarkers Working Group: Part 2: TILs in Melanoma, Gastrointestinal Tract Carcinomas, Non-Small Cell Lung Carcinoma and Mesothelioma, Endometrial and Ovarian Carcinomas, Squamous Cell Carcinoma of the Head and Neck, Genitourinary Carcinomas, and Primary Brain Tumors. *Adv Anat Pathol*. 2017;24:311-35.

38. Sobottka B, Nowak M, Frei AL, et al. Establishing standardized immune phenotyping of metastatic melanoma by digital pathology. *Lab Invest*. 2021;101:1561-70.

39. Park CK, Kim SK. Clinicopathological significance of intratumoral and peritumoral lymphocytes and lymphocyte score based on the histologic subtypes of cutaneous melanoma. *Oncotarget*. 2017;8:14759-69.

40. Morrison C, Pabla S, Conroy JM, et al. Predicting response to checkpoint inhibitors in melanoma beyond PD-L1 and mutational burden. *J Immunother Cancer*. 2018;6:32.

41. Indini A, Massi D, Pirro M, et al. Targeting inflamed and non-inflamed melanomas: biological background and clinical challenges. *Semin Cancer Biol*. 2022;86:477-90.

42. Ledderose S, Ledderose C, Penkava J, et al. Prognostic Value of Tumor-Infiltrating Lymphocytes in Sinonasal Mucosal Melanoma. *Laryngoscope*. 2022;132:1334-9.

43. Ledderose S, Schulz H, Paul T, et al. Characterization of the tumor-infiltrating lymphocyte landscape in sinonasal mucosal melanoma. *Pathol Res Pract*. 2023;241:154289.

44. Teng MWL, Ngiow SF, Ribas A, et al. Classifying Cancers Based on T-cell Infiltration and PD-L1. *Cancer Res*. 2015;75:2139-45.

45. Cristescu R, Mogg R, Ayers M, et al. Pan-tumor genomic biomarkers for PD-1 checkpoint blockade-based immunotherapy. *Science*. 2018;362:eaar3593.

46. NCCN Clinical Practice Guidelines in Oncology (NCCN Guidelines®). Melanoma: Cutaneous Version 2.2023.

47. Lopez F, Rodrigo JP, Cardesa A, et al. Update on primary head and neck mucosal melanoma. *Head Neck*. 2016;38(1):147-55.

48. Jeong YJ, Thompson JF, Ch'ng S. Epidemiology, staging and management of mucosal melanoma of the head and neck: a narrative review. *Chin Clin Oncol*. 2023;12(3):28.

49. Ascierto PA, Accorona R, Botti G, et al. Mucosal melanoma of the head and neck. *Crit Rev Oncol Hematol*. 2017;112:136-52.

50. Harms PW, Frankel TL, Moutafi M, et al. Multiplex Immunohistochemistry and Immunofluorescence: A Practical Update for Pathologists. *Mod Pathol*. 2023;36:100197.

51. Ugolini F, Pasqualini E, Simi S, et al. Bright-Field Multiplex Immunohistochemistry Assay for Tumor Microenvironment Evaluation in Melanoma Tissues. *Cancers (Basel)*. 2022;14:3682.

52. Lu S, Stein JE, Rimm DL, et al. Comparison of Biomarker Modalities for Predicting Response to PD-1/PD-L1 Checkpoint Blockade: A Systematic Review and Meta-analysis. *JAMA Oncol*. 2019;5:1195-204.

53. Loree TR, Mullins AP, Spellman J, et al. Head and neck mucosal melanoma: a 32-year review. *Ear Nose Throat J*. 1999;78:372-5.

54. Roth TN, Gengler C, Huber GF, et al. Outcome of sinonasal melanoma: clinical experience and review of the literature. *Head Neck*. 2010;32:1385-92.

55. Rinaldo A, Shaha AR, Patel SG, et al. Primary mucosal melanoma of the nasal cavity and paranasal sinuses. *Acta Otolaryngol*. 2001;121:979-82.

56. Femiano F, Lanza A, Buonaiuto C, et al. Oral malignant melanoma: a review of the literature. *J Oral Pathol Med*. 2008;37:383-8.

57. Guevara-Canales JO, Gutiérrez-Morales MM, Sacsaquispe-Contreras SJ, et al. Malignant melanoma of the oral cavity. Review of the literature and experience in a Peruvian population. *Med Oral Patol Oral Cir Bucal*. 2012;17:e206–e211.

58. Wenig BM. Laryngeal mucosal malignant melanoma. A clinicopathologic, immunohistochemical, and ultrastructural study of four patients and review of the literature. *Cancer*. 1995;75:1568-77.

59. Terada T, Saeki N, Toh K, et al. Primary malignant melanoma of the larynx: a case report and literature review. *Auris Nasus Larynx*. 2007;34:105-10.

60. Thoeny HC, De Keyzer F, King AD. Diffusion-weighted MR imaging in the head and neck. *Radiology*. 2012;263:19-32.

61. Kim SS, Han MH, Kim JE, et al. Malignant melanoma of the sinonasal cavity: explanation of magnetic resonance signal intensities with histopathologic characteristics. *Am J Otolaryngol*. 2000;21:366-78.

62. Ricci C, Dika E, Ambrosi F, et al. Cutaneous Melanomas: A Single Center Experience on the Usage of Immunohistochemistry Applied for the Diagnosis. *Int J Mol Sci*. 2022;23:5911.

63. Ricci C, Altavilla MV, Corti B, et al. PRAME Expression in Mucosal Melanoma of the Head and Neck Region. *Am J Surg Pathol*. 2023;47:599-610.

64. Raghavan SS, Wang JY, Kwok S, et al. PRAME expression in melanocytic proliferations with intermediate histopathologic or spitzoid features. *J Cutan Pathol*. 2020;47:1123-31.

65. Scheurleer WFJ, Braunius WW, Tijink BM, et al. PRAME Staining in Sinonasal Mucosal Melanoma: A Single-Center Experience. *Head Neck Pathol*. 2023;17:401-8.

66. Hovander D, Allen J, Oda D, et al. PRAME immunohistochemistry is useful in the diagnosis of oral malignant melanoma. Oral Oncol. 2022;124:105500.

67. Cascardi E, Cazzato G, Ingravallo G, et al. PReferentially Expressed Antigen in MElanoma (PRAME): preliminary communication on a translational tool able to early detect Oral Malignant Melanoma (OMM). *J Cancer*. 2023;14:628-33.

68. Amin MB, Edge S, Greene F, et al. *AJCC Cancer Staging Manual*, 8th ed. Springer; 2017.

69. Lechner M, Takahashi Y, Turri-Zanoni M, et al. International Multicenter Study of Clinical Outcomes of Sinonasal Melanoma Shows Survival Benefit for Patients Treated with Immune Checkpoint Inhibitors and Potential Improvements to the Current TNM Staging System. *J Neurol Surg B Skull Base*. 202;84:307-19.

70. Patel SG, Lydiatt WM. Staging of head and neck cancers: is it time to change the balance between the ideal and the practical? *J Surg Oncol*. 2008;97:653-7.

71. Farber NI, Bavier RD, Crippen MM, et al. Comparing endoscopic resection and open resection for management of sinonasal mucosal melanoma. *Int Forum Allergy Rhinol*. 2019;9:1492-8.

72. Swegal W, Koyfman S, Scharpf J, et al. Endoscopic and open surgical approaches to locally advanced sinonasal melanoma: comparing the therapeutic benefits. *JAMA Otolaryngol Head Neck Surg*. 2014;140:840-5.

73. Strojan P. Role of radiotherapy in melanoma management. *Radiol Oncol*. 2010;44:1-12.

74. Grant-Freemantle MC, Lane O'Neill B, Clover AJP. The effectiveness of radiotherapy in the treatment of head and neck mucosal melanoma: Systematic review and meta-analysis. *Head Neck*. 2021;43:323-33.

75. Li W, Yu Y, Wang H, et al. Evaluation of the prognostic impact of postoperative adjuvant radiotherapy on head and neck mucosal melanoma: a meta-analysis. *BMC Cancer*. 2015;15:758.

76. Zenda S, Akimoto T, Mizumoto M, et al. Phase II study of proton beam therapy as a nonsurgical approach for mucosal melanoma of the nasal cavity or para-nasal sinuses. *Radiother Oncol*. 2016;118:267-71.

77. Serrone L, Zeuli M, Sega FM, et al. Dacarbazine-based chemotherapy for metastatic melanoma: thirty-year experience overview. *J Exp Clin Cancer Res*. 2000;19:21-34.

78. Lian B, Si L, Cui C, et al. Phase II randomized trial comparing high-dose IFN-α2b with temozolomide plus cisplatin as systemic adjuvant therapy for resected mucosal melanoma. *Clin Cancer Res*. 2013;19:4488-98.

79. Bin Lian B, Lu Si L, Chuanliang Cui C, et al. Phase II randomized trial comparing high-dose IFN-α2b with temozolomide plus cisplatin as systemic adjuvant therapy for resected mucosal melanoma. *Clin Cancer Res*. 2013;19(16):4488-98.

80. Steeb T, Wessely A, Petzold A, et al. c-Kit inhibitors for unresectable or metastatic mucosal, acral or chronically sun-damaged melanoma: a systematic review and one-arm meta-analysis. *Eur J Cancer*. 2021;157:348-57.

81. Tyrrell H, Payne M. Combatting mucosal melanoma: recent advances and future perspectives. Melanoma Manag. 2018;5:MMT11.

82. Schuler M, Zimmer L, Kim KB, et al. Phase Ib/II Trial of Ribociclib in Combination with Binimetinib in Patients with NRAS-mutant Melanoma. *Clin Cancer Res*. 2022;28:3002-10.

83. Sheng X, Yan X, Chi Z, et al. Axitinib in Combination With Toripalimab, a Humanized Immunoglobulin G4 Monoclonal Antibody Against Programmed Cell Death-1, in Patients With Metastatic Mucosal Melanoma: An Open-Label Phase IB Trial. *J Clin Oncol*. 2019;37:2987-99.

84. Robert C, Thomas L, Bondarenko I, et al. Ipilimumab plus dacarbazine for previously untreated metastatic melanoma. *N Engl J Med*. 2011;364:2517-26.

85. Topalian SL, Sznol M, McDermott DF, et al. Survival, durable tumor remission, and long-term safety in patients with advanced melanoma receiving nivolumab. *J Clin Oncol*. 2014;32:1020-30.

86. Urba WJ, Martín-Algarra S, Callahan M, et al. Immunomodulatory activity of nivolumab monotherapy in patients with advanced melanoma. *Cancer Res*. 2015;75:2855.

87. Robert C, Long GV, Brady B, et al. Nivolumab in previously untreated melanoma without BRAF mutation. *N Engl J Med*. 2015;372:320-30.

88. Weber JS, D'Angelo SP, Minor D, et al. Nivolumab versus chemotherapy in patients with advanced melanoma who progressed after anti-CTLA-4 treatment (CheckMate 037): a randomised, controlled, open-label, phase 3 trial. *Lancet Oncol*. 2015;16:375-84.

89. Shoushtari AN, Wagstaff J, Ascierto PA, et al. CheckMate 067: Long-term outcomes in patients with mucosal melanoma. *J Clin Oncol*. 2020;38:10019.

90. Eggermont AM, Chiarion-Sileni V, Grob JJ, et al. Prolonged Survival in Stage III Melanoma with Ipilimumab Adjuvant Therapy. *N Engl J Med*. 2016;375:1845-55.

91. Lian B, Si L, Cui C, et al. Phase II randomized trial comparing high-dose IFN-α2b with temozolomide plus cisplatin as systemic adjuvant therapy for resected mucosal melanoma. *Clin Cancer Res*. 2013;19:4488-98.

92. Ascierto PA, Del Vecchio M, Mandalá M, et al. Adjuvant nivolumab versus ipilimumab in resected stage IIIB-C and stage IV melanoma (CheckMate 238): 4-year results from a multicentre, double-blind, randomised, controlled, phase 3 trial. *Lancet Oncol*. 2020;21:1465-77.

93. Amaria RN, Reddy SM, Tawbi HA, et al. Neoadjuvant immune checkpoint blockade in high-risk resectable melanoma. *Nat Med*. 2018;24:1649-54.

94. Cui C, Wang X, Lian B, et al. A phase 2 clinical trial of neoadjuvant anti-PD-1 ab (Toripalimab) plus axitinib in resectable mucosal melanoma. *J Clin Oncol*. 2021;39:9512.

95. Ho J, Mattei J, Tetzlaff M, et al. Neoadjuvant checkpoint inhibitor immunotherapy for resectable mucosal melanoma. *Front Oncol*. 2022;12:1001150.

96. Rager T, Eckburg A, Patel M, et al. Treatment of Metastatic Melanoma with a Combination of Immunotherapies and Molecularly Targeted Therapies. *Cancers (Basel)*. 2022;14:3779.

97. Dika E, de Biase D, Lambertini M, et al Mutational landscape in squamous cell carcinoma of the nail unit. *Exp Dermatol*. 2022;31:854-61.

98. de Biase D, Acquaviva G, Visani M, et al. Molecular Diagnostic of Solid Tumor Using a Next Generation Sequencing Custom-Designed Multi-Gene Panel. *Diagnostics (Basel)*. 2020;23;10:250.

99. Kopanos C, Tsiolkas V, Kouris A, et al. VarSome: the human genomic variant search engine. *Bioinformatics*. 2019;35:1978-80.

100. Ricci C, Righi A, Ambrosi F, et al. Prognostic Impact of MCPyV and TIL Subtyping in Merkel Cell Carcinoma: Evidence from a Large European Cohort of 95 Patients. *Endocr Pathol*. 2020;31:21-32.

101. Melotti S, Ambrosi F, Franceschini T, et al. TAMs PD-L1(+) in the reprogramming of germ cell tumors of the testis. *Pathol Res Pract*. 2023;247:154540.

102. Ugolini F, De Logu F, Iannone LF, et al. Tumor infiltrating lymphocytes recognition in primary melanoma by deep learning convolutional neural network. *Am J Pathol*. 2023 Sep 19;S0002-9440(23)00324-3. DOI: 10.1016/j.ajpath.2023.08.013. *Online ahead of print*.

103. Galon J, Costes A, Sanchez-Cabo F, et al. Type, density, and location of immune cells within human colorectal tumors predict clinical outcome. *Science*. 2006;313:1960-4.

104. Rindi G, Klöppel G, Alhman H, et al. TNM staging of foregut (neuro)endocrine tumors: a consensus proposal including a grading system. *Virchows Arch*. 2006;449:395-401.

105. Fattore L, Ruggiero CF, Liguoro D, et al. Single cell analysis to dissect molecular heterogeneity and disease evolution in metastatic melanoma. *Cell Death Dis*. 2019;10:827.

106. Shannan B, Perego M, Somasundaram R, et al. Heterogeneity in Melanoma. *Cancer Treat Res*. 2016;167:1-15.

107. Wilmott JS, Tembe V, Howle JR, et al. Intratumoral molecular heterogeneity in a BRAF-mutant, BRAF inhibitor-resistant melanoma: a case illustrating the challenges for personalized medicine. *Mol Cancer Ther*. 2012;11:2704-8.

12 Abbreviations

mucosal melanoma of the head and neck region (MM-H&N); bright-field multiplex immunohistochemistry (BF-mIHC); tumor microenvironment (TME); mucosal melanoma (MM); nasal cavity/nasal septum/turbinates (NC/NS/T); wild-type status (WT); tumor-infiltrating lymphocytes (TILs); tumor-associated macrophages (TAMs); immune checkpoint inhibitors (ICIs); programmed death-ligand 1 (PD-L1); tumor mutational burden (TMB); gene expression profile (GEP); National Comprehensive Cancer Network (NCCN); overall survival (OS); 5-year survival (5y-S); multiplex immunofluorescence (mIHF); magnetic resonance imaging (MRI); World Health Organization (WHO); American Joint Committee on Cancer (AJCC); interferon (IFN); recurrence-free survival (RFS); anti-cytotoxic T-lymphocyte antigen 4 (anti-CTLA-4); lympho-vascular invasion (LVI); perineural infiltration (PNI); American College of Medical Genetics and Genomics (ACMG); formalin-fixed paraffin-embedded (FFPE); hematoxylin and eosin (H&E); next-generation sequencing (NGS); high-power fields (HPF); excision of the primary tumor (EPT); excision of local recurrence/residual tumor (ELR/RT); incisional biopsy (IB); nodular (N); mucosal lentiginous (ML); not evaluable (NE); variant allele frequency (VAF); pathogenic (Path); likely pathogenic (Likely Path); variant of unknown significance (VUS).


ALMA MATER STUDIORUM
UNIVERSITÀ DI BOLOGNA